

Using Annealed Pyrolytic Graphite in Conduction Cooled Electronics Cooling
Applications

By

Shane B Flynn, P. Eng.

A thesis is submitted to
the Faculty of Graduate Studies and Research
in partial fulfillment of
the requirements of the degree of

Master of Applied Science

Ottawa Carleton Institute for Mechanical and Aerospace Engineering
Faculty of Engineering
Department of Mechanical and Aerospace Engineering
Carleton University
Ottawa, Ontario, Canada, K1S 5B6

© Copyright 2005, Shane B Flynn, P. Eng.



Library and
Archives Canada

Bibliothèque et
Archives Canada

Published Heritage
Branch

Direction du
Patrimoine de l'édition

395 Wellington Street
Ottawa ON K1A 0N4
Canada

395, rue Wellington
Ottawa ON K1A 0N4
Canada

Your file *Votre référence*
ISBN: 978-0-494-16457-0
Our file *Notre référence*
ISBN: 978-0-494-16457-0

NOTICE:

The author has granted a non-exclusive license allowing Library and Archives Canada to reproduce, publish, archive, preserve, conserve, communicate to the public by telecommunication or on the Internet, loan, distribute and sell theses worldwide, for commercial or non-commercial purposes, in microform, paper, electronic and/or any other formats.

The author retains copyright ownership and moral rights in this thesis. Neither the thesis nor substantial extracts from it may be printed or otherwise reproduced without the author's permission.

AVIS:

L'auteur a accordé une licence non exclusive permettant à la Bibliothèque et Archives Canada de reproduire, publier, archiver, sauvegarder, conserver, transmettre au public par télécommunication ou par l'Internet, prêter, distribuer et vendre des thèses partout dans le monde, à des fins commerciales ou autres, sur support microforme, papier, électronique et/ou autres formats.

L'auteur conserve la propriété du droit d'auteur et des droits moraux qui protègent cette thèse. Ni la thèse ni des extraits substantiels de celle-ci ne doivent être imprimés ou autrement reproduits sans son autorisation.

In compliance with the Canadian Privacy Act some supporting forms may have been removed from this thesis.

Conformément à la loi canadienne sur la protection de la vie privée, quelques formulaires secondaires ont été enlevés de cette thèse.

While these forms may be included in the document page count, their removal does not represent any loss of content from the thesis.

Bien que ces formulaires aient inclus dans la pagination, il n'y aura aucun contenu manquant.


Canada

Table of Contents

List of Figures	vi
List of Abbreviations	ix
Abstract	x
1 Introduction.....	1-1
1.1 Commercial Electronics.....	1-1
1.2 Rugged Electronics.....	1-2
1.2.1 Automotive/Industrial	1-3
1.2.2 Space.....	1-4
1.2.3 Military.....	1-4
1.3 Evolution of Conduction Cooled Electronics - Industry Perspective	1-5
1.4 Objective	1-12
1.5 Approach.....	1-13
2 Background	2-1
2.1 Heat Transfer in Electronics Cooling.....	2-1
2.1.1 Isotropic Materials	2-3
2.1.2 Laminates.....	2-3
2.1.3 Heat Pipes	2-5
2.1.4 Composites.....	2-6

3	Annealed Pyrolytic Graphite	3-1
3.1	Introduction to Annealed Pyrolytic Graphite	3-1
3.2	Physical properties	3-2
3.3	Industry Experience	3-3
4	Thermal Analysis	4-5
4.1	Background	4-5
4.2	Frame Finite Element Model	4-6
4.2.1	Geometry/Boundary Conditions/Heat Loads	4-8
4.2.2	Material Properties	4-8
4.2.3	Design studies/Sensitivity Analysis	4-11
4.2.4	Assumptions	4-12
4.2.5	Results	4-15
4.2.5.1	APG Location	4-16
4.2.5.2	APG Orthogonal Thermal Conductivity	4-19
4.2.5.3	APG Thickness	4-20
4.2.5.4	APG In-plane Thermal Conductivity	4-21
4.2.6	Discussion	4-22
5	Fabrication	5-26
5.1	General Fabrication Method	5-26
5.2	Fabrication Issues	5-28

6	Experimental Test.....	6-1
6.1	Thermal Frame Testing	6-1
6.1.1	Test Specimens	6-1
6.1.2	Test Setup.....	6-3
6.1.3	Assumptions.....	6-7
6.1.4	Test Sequence	6-8
6.1.5	Results	6-9
6.1.5.1	Constant Ambient Temperature	6-9
6.1.5.2	Varying Ambient Temperature	6-11
6.1.6	Discussion.....	6-13
6.2	Sectioned Sample Testing	6-19
6.2.1	Test Specimen	6-19
6.2.2	Test Setup and Procedure	6-21
6.2.3	Discussion.....	6-21
6.3	Industry Experience.....	6-21
6.4	Conclusions	6-22
7	Other Environmental/ Mechanical Considerations.....	7-1
7.1	Environmental Considerations	7-1
7.2	Mechanical Property Considerations	7-6
8	Conclusions and Recommendations.....	8-1

8.1 Conclusions8-1

8.2 Recommendations8-2

APPENDIX A University of Waterloo Thermal Conductivity Test Report. I

List of Figures

Figure 1: CCA Utilizing Heat Ladder Cooling Scheme (Component Side)	1-6
Figure 2: CCA Utilizing Heat Ladder Cooling Scheme (Solder Side).....	1-7
Figure 3: CCA Utilizing Combined Heat Ladder and PWB Core Cooling Scheme (Component Side).....	1-8
Figure 4: CCA Utilizing Combined Heat Ladder and PWB Core Cooling Scheme (Solder Side).....	1-9
Figure 5: CCA Utilizing Combined PWB Core and External Frame Cooling Scheme (Component Side).....	1-10
Figure 6: CCA Utilizing Combined PWB Core and External Frame Cooling Scheme (Solder Side).....	1-10
Figure 7: CCA Mezzanine Card used for Functionally Expansion (Component Side)	1-11
Figure 8: CCA Mezzanine Card used for Functionally Expansion (Solder Side).....	1-12
Figure 9: Top View of Finite Element Model	4-7
Figure 10: Bottom View of Finite Element Model.....	4-7
Figure 11: In-plane APG Thermal Conductivity	4-10
Figure 12: FEA Results of Analysis Case 1, All Aluminum Frame, 40 W.....	4-16

Figure 13: FEA Results of Analysis Case 2, APG Mid and Side Sections, 40 W.4-17

Figure 14: FEA Results of Analysis Case 3, APG Mid-Section, 40 W.....4-18

Figure 15: FEA Results of Analysis Case 4, APG Side-Sections, 40 W.....4-19

Figure 16: FEA Results of Analysis Case 5, APG, 20 W/m K Thru-Plane, 40 W.....4-20

Figure 17: FEA Results of Analysis Case 6, 0.040” Thick APG, 40 W.4-21

Figure 18: FEA Results of Analysis Case 7, 0.040” Thick APG, 1200 W/m K, 40 W....4-22

Figure 19: Aluminum Thermal Frame with Black Anodize Surface Finish6-2

Figure 20: APG/Aluminum Composite Thermal Frame (Mid-Section APG Visible)...6-2

Figure 21: APG/Aluminum Composite Thermal Frame Cross-Section (APG Inserts Visible)6-3

Figure 22: Test Specimens Installed in Test Fixture6-5

Figure 23: Test Specimens Installed in Test Fixture and Surrounded with Insulation...6-5

Figure 24: Test Specimens Installed in Test Fixture with Covers Installed6-6

Figure 25: Composite (Raw Aluminum finish) and All-Aluminum (Black Anodized Finish) Frames with Heater Elements and Thermocouples Attached6-6

Figure 26: Thermal Test Results for Al and APG/Al Test Specimens at Room Ambient Temperature with Varying Power Dissipation6-11

Figure 27: Aluminum Test Specimen Results with Varying Ambient Temperature ...6-12

Figure 28: APG/Al Test Specimen Results with Varying Ambient Temperature.....6-13

Figure 29: Comparison of FEA and Test Results.....6-14

Figure 30: Corrected APG FEA Results.....6-16

Figure 31: Effect of In-Plane Thermal Conductivity on APG Thermal Results at 40 W.6-17

Figure 32: APG Thermal Test Results with Varying Ambient Temperature6-18

Figure 33: APG Composite Prototype 2 with Sections Removed.....6-20

Figure 34: APG Sections Removed From Prototype.....6-20

Figure 35: APG Section Laminated Together, Two Thicknesses of APG6-20

Figure 36: Sine Sweep Response, All Aluminum Frame (2 g input, 15-2000 Hz)7-2

Figure 37: Sine Sweep Response, APG/Aluminum Frame #1 (2 g input, 15-2000 Hz) 7-2

Figure 38: Sine Sweep Response, APG/Aluminum Frame #2 (2 g input, 15-2000 Hz) 7-3

Figure 39: Random Vibration Response, All Aluminum Frame (0.1 g²/Hz, 15-2000 Hz)7-3

Figure 40: Random Vibration Response, APG/Aluminum Frame #1 (0.1 g²/Hz, 15-2000 Hz)7-4

Figure 41: Random Vibration Response, APG/Aluminum Frame #2 (0.1 g²/Hz, 15-2000 Hz) 7-4

List of Abbreviations

ANSI	American National Standard Institute
APG	Annealed Pyrolytic Graphite
CCA	Circuit Card Assembly
COTS	Commercial Off The Shelf
CWCEC	Curtiss-Wright Control – Embedded Computing
DMV	Dy 4 Military VME
DSP	Digital Signal Processor
FEA	Finite Element Analysis
FEM	Finite Element Model
IEEE	Institute of Electrical and Electronics Engineers
PCI	Peripheral Component Interconnect
PMC	PCI Mezzanine Card
PSD	Power Spectral Density
PWB	Printed Wiring Board
RMS	Root Mean Square
SBC	Single Board Computer
UUT	Unit Under Test
VITA	VME Industry Trade Association
VME	Versa Modules Eurocard

Abstract

In this study, the thermal performance of an Annealed Pyrolytic Graphite (APG)/aluminum composite material has been investigated for use in the design and manufacture of a conduction-cooled electronics thermal frame. The frame design utilized several inserts of APG of different thicknesses embedded within an aluminum parent material to provide a high thermal conductivity composite material to increase conduction heat transfer rates.

Finite Element Analysis (FEA) was used to examine several design trade-offs and material property considerations such as the in-plane thermal conductivity, thru-plane thermal conductivity and thickness of the APG inserts. The results of the FEA indicated a significant improvement in thermal performance of the composite material when directly compared with an equivalent all aluminum design.

In an attempt to confirm the results of the thermal analysis, prototype frames were manufactured and subjected to thermal testing in a manner to mimic the conditions of the FEA. The results of the thermal testing reveal that the composite material does not perform as well as anticipated and the effective thermal conductivity of the APG material was estimated by calibrating the results of the test to the FEA using the all aluminum design as a control and correcting for parasitic heat loss from the test set up.

Results indicate that the actual effective thermal conductivity of the APG material lies in the range of approximately 640 – 950 W/m K compared to a reported value of 1530

W/m K according to the manufacturer. However, this value of thermal conductivity proved to still provide a significant improvement in thermal performance of the APG/aluminum composite design when compared to the all aluminum design.

1

Introduction

The electronics industry, while still relatively young, has grown in leaps and bounds with the past three of four decades. Electronics cooling has been a necessary by product of the electronics industry for nearly as long whether through the cooling of vacuum tubes or complex integrated circuits. In the 1970's Dr. Gordon Moore predicted that semiconductor transistor density and performance would continue to double approximately every 18 months, this prediction became known as Moore's Law. Thus far, that prediction has proven to be true¹. As transistor density increases and feature size decreases the heat flux of these devices increases exponentially resulting in a rising challenge for thermal engineers. Where a flux of 1 to 5 W/cm² was the norm fifteen years ago, 10 to 50 W/cm² is not unheard of today. Conventional means of cooling electronics are becoming obsolete while more exotic solutions are gaining acceptance.

1.1 Commercial Electronics

The vast majority of electronics produced today are for commercial consumer consumption. Home personal computers, mobile laptops, cellular telephones and other handhold devices account for a large percentage of the market. The demands of consumers for faster, more powerful, feature rich products are driving the technology to new levels of complexity and higher power dissipation. Personal computer processors traditionally used passive heat sink technology and natural convection heat transfer that

evolved to fan-assisted heat sinks and forced convection heat transfer. Today, it is possible to purchase PC chassis' with built-in refrigeration units. Most modern laptop computers utilize heat pipe technology and some high-end supercomputer mainframes have utilized liquid cooling.

While the electronics industry has made large strides in technology, the electronics cooling industry has lagged behind with solutions that will meet the cooling needs of today's and the futures electronics technology. Luckily some trends in electronics technology help to alleviate this problem such as shrinking feature size and decreased operating voltages which result in lower power per gate per MHz values (W/Gate/MHz), however, the exponential increase in the number of gates and speed of processors still imposes a sharp overall increase in the heat flux of devices.

The vast majority of commercial electronics utilizes convection cooling (both natural and forced) as a primary means of heat transfer. Some exotic applications utilize fluids other than air to increase overall heat transfer coefficients.

1.2 Rugged Electronics

The thermal challenges of commercial electronics environments can pale in comparison to those applications where the operating environmental conditions are more demanding. Where commercial applications often have operating environments that include ambient temperatures of 0 to 70°C, little to no mechanical shock or vibration, and relatively clean air quality, rugged electronics may face temperature extremes greater than -55 to +125°C, harsh shock and vibration, and corrosive environments. In addition to these

environmental challenges, rugged electronics are often faced with packaging challenges, harsher reliability requirements and mission critical roles that require more attention to the overall mechanical design.

Many examples of rugged electronics applications can be found in automotive, industrial, space, and military applications. Fortunately, a greater percentage of product cost is often spent on electronics cooling and overall mechanical design in these applications when compared with commercial applications.

1.2.1 Automotive/Industrial

In the past 25 years the value of the electronics components in the average vehicle has increased from \$110 to \$1,510². The environment that these electronics must operate in is corrosive, experiences high levels of shock and vibration and results in temperatures that range from -40 to +125°C. Some automotive electronics categories include Engine and power train, chassis and safety, comfort and convenience, display and audio as well as signal communications and wiring harnesses. These electronics must not only work but must work reliably for an extended period of time, greater than 10 years is expected; therefore electronics cooling technology is critical.

Industrial electronics applications are similar to automotive in terms of operating environment. They include such applications as heavy machinery, oil exploration and mining.

While all three modes of heat transfer are utilized in automotive and industrial applications, conduction heat transfer plays a primary role in the transfer of heat from components to heat rejection devices.

1.2.2 Space

Electronics have been used in space from the very first satellite put in to orbit. These electronics face unique challenges such as extreme thermal cycling, high levels of radiation, severe shock and vibration and the absence of air for convection cooling. These electronics experience high heat flux through radiation from the sun but reject heat through radiation to the darkness of space. While radiation is the primary rejection mode of heat transfer, conduction is used to transport heat from electronics components to the radiation surface.

1.2.3 Military

In 1970 the military accounted for 10% of the electronics market share, by 2000 that market share dwindled to less than 0.1%³. In 1994 former US Secretary of Defense William Perry declared an initiative to increase the use of commercial-off-the-shelf technology. As a result of the drastically reduced military demand on the electronics industry to produce high-temperature hermetic electronics packages and the military's desire to use the latest and greatest processing technology, the use of commercial electronics in military applications took root.

Military electronics applications demand the harshest environment with extreme temperatures, harsh environmental conditions such as salt atmosphere, radiation, humidity, corrosive fluids and high level so shock and vibration. Military applications require high level of reliability in mission critical scenarios and are expected to be in service for 10 – 30 years. Under these circumstances cooling is extremely important. Many military applications rely on conduction cooling of devices within a sealed enclosure to an external heat sink, which may be the chassis of a tank or liquid cooled avionics rack.

Current military electronics cooling is approaching its limit in terms of allowable heat flux. One of the limiting factors is the conduction thermal resistance of the structures used to cool these electronics. This thesis aims to address that limit.

1.3 Evolution of Conduction Cooled Electronics - Industry Perspective

Although conduction cooling is not exclusive to the military, it is the predominant form of heat transfer used for electronics cooling in many rugged military applications. While custom standards and physical form factors are used frequently in military applications, several commercial and industry standards are also used for the design of military electronics; some of these include SEM-E, VME and CompactPCI. For nearly 20 years, CWCEC, the employer of the author, has been designing and manufacturing rugged electronics in these standard form factors as well as custom designed modules.

As electronics packaging evolved and power dissipation trends increase, the method of employing conduction cooling has evolved. Early designs consisted of printed circuit

boards (PCBs) with through-hole components that were conduction cooled through the use of an aluminum structure bonded to the surface of the PCB. The through hole components were then assembled to this structure, soldered to the PCB and bonded to the aluminum structure which was used as the primary conduction heat transfer path. This aluminum structure is often referred to as a “heat ladder”. The components were thereby cooled through conduction in the heat ladder to the circuit card edges. This design concept is illustrated in Figure 1 and Figure 2.

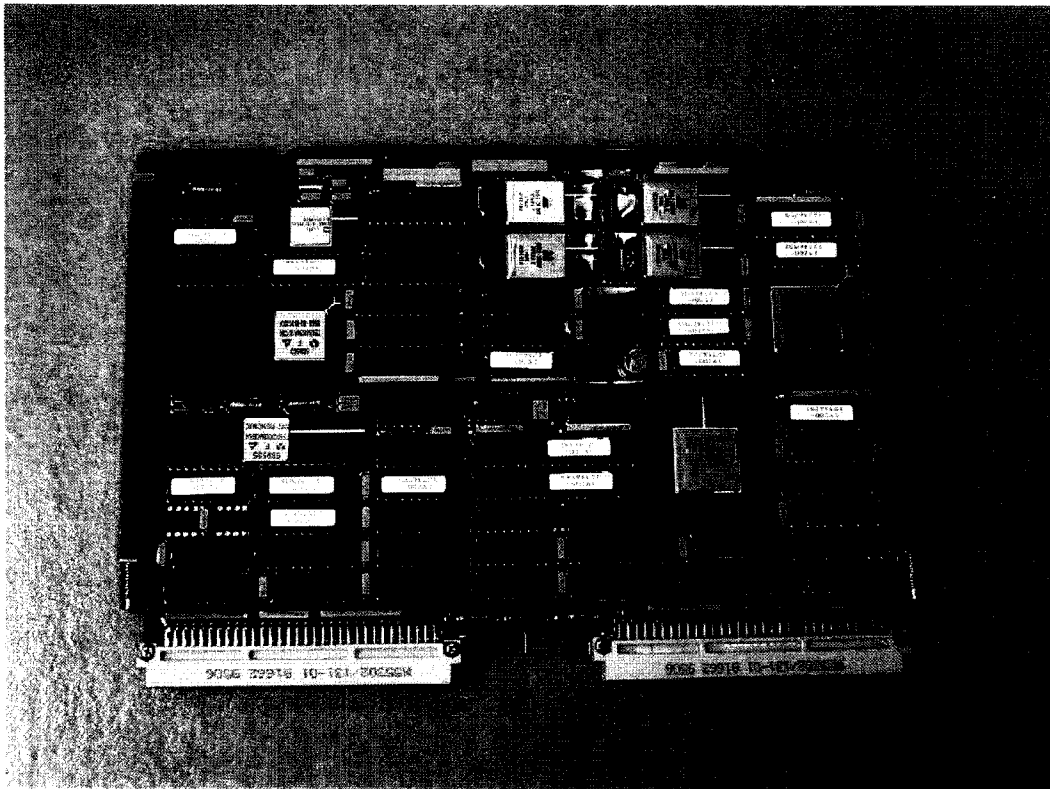


Figure 1: CCA Utilizing Heat Ladder Cooling Scheme (Component Side)

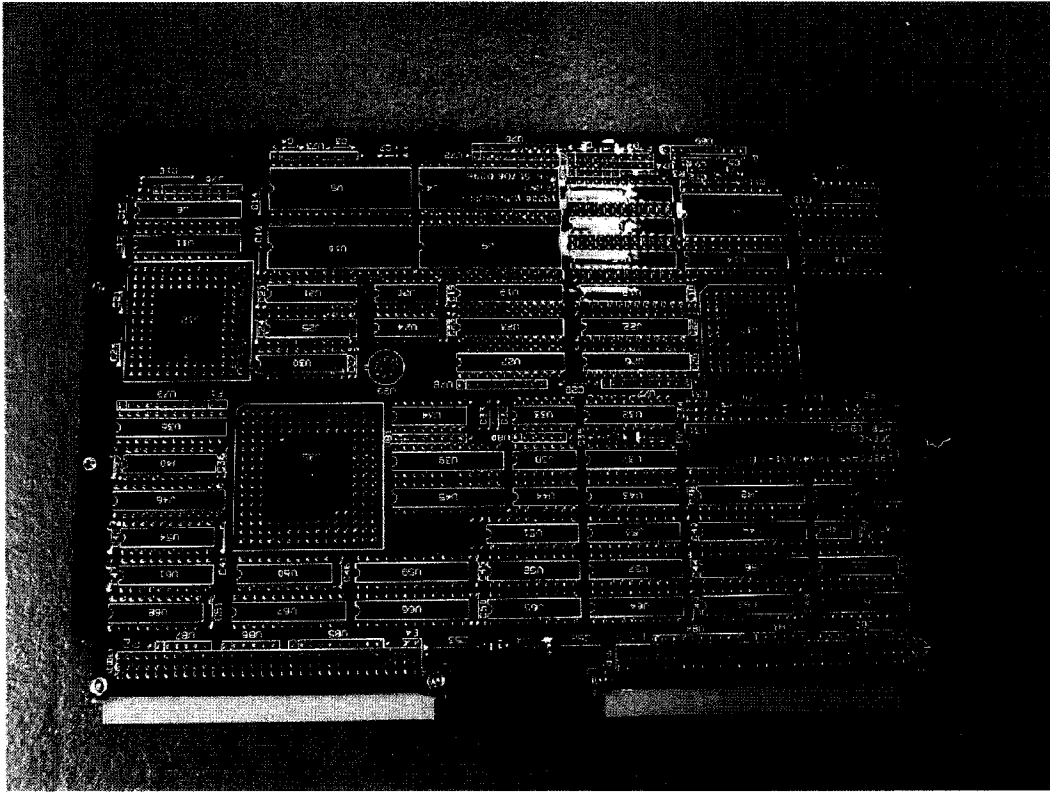


Figure 2: CCA Utilizing Heat Ladder Cooling Scheme (Solder Side)

With the adoption of surface mount components and especially fine pitch devices and Ball Grid Arrays (BGAs), the heat ladder design became impractical and obsolete. A method of conduction cooling these devices involved adding thick layers of copper to the PCB laminate structure as internal layers. This resulted in a PCB with relatively high thermal conductivity. For example, typical FR-4 Epoxy laminate has a thermal conductivity of 0.3 W/m K, however, with the addition of thick layers of copper (typically 8 – 12 total ounces of thickness, where one ounce equals approximately 1.4 mils), the equivalent thermal conductivity of the PCB is in the range of approximately 60 – 90 W/m K depending on total PCB thickness using a weighted average of copper and FR-4 Epoxy. This technique of using the PCS as the primary conduction heat

transfer path was often referred to as “core cooling”. This design concept is illustrated in Figure 3 and Figure 4.

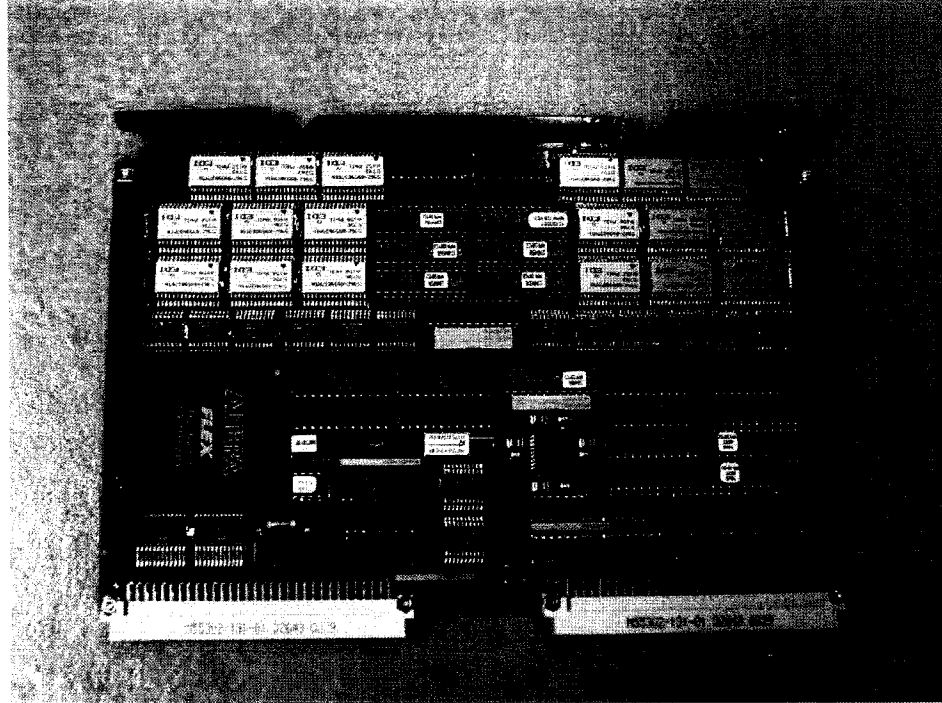


Figure 3: CCA Utilizing Combined Heat Ladder and PWB Core Cooling Scheme (Component Side)

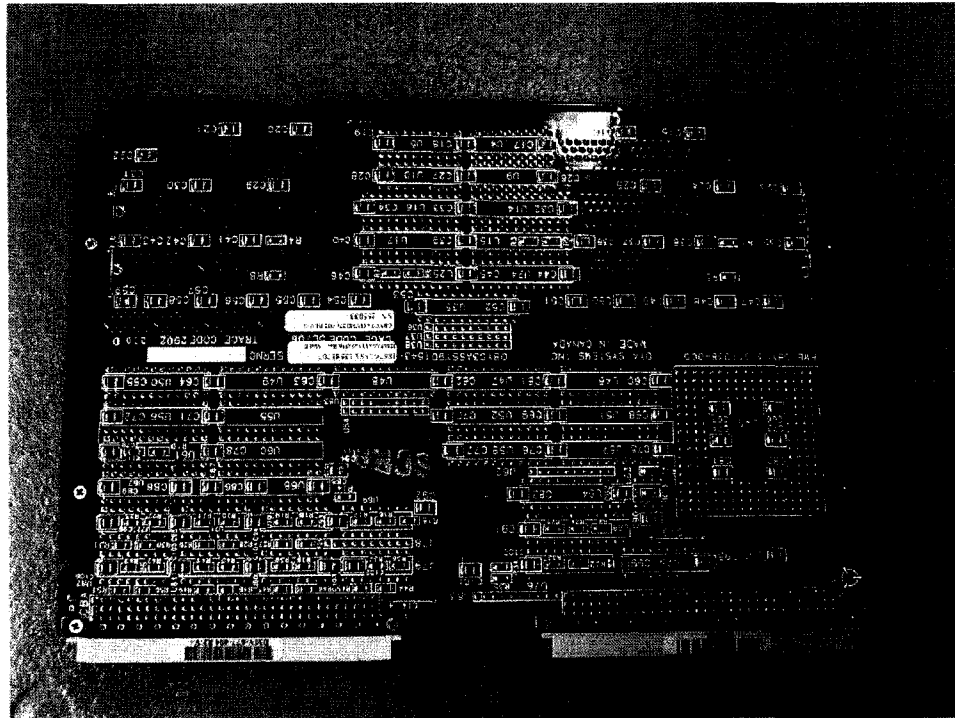


Figure 4: CCA Utilizing Combined Heat Ladder and PWB Core Cooling Scheme (Solder Side)

A similar idea employed the use of a dedicated metal core sandwiched between two PCBs, however, in this case the metal core was not manufactured as an integral part of the PCB.

The ever increasing heat flux density of circuit card designs have rendered the core cooling methodology incapable of handling the cooling needs of designs within the past several years. Many modern circuit card designs utilize core cooling in combination with additional direct cooling of high power dissipation devices such as processors. These devices are often directly shunted to aluminum structures that are attached to the circuit card over the top of components. This design concept is illustrated in Figure 5 and Figure 6.

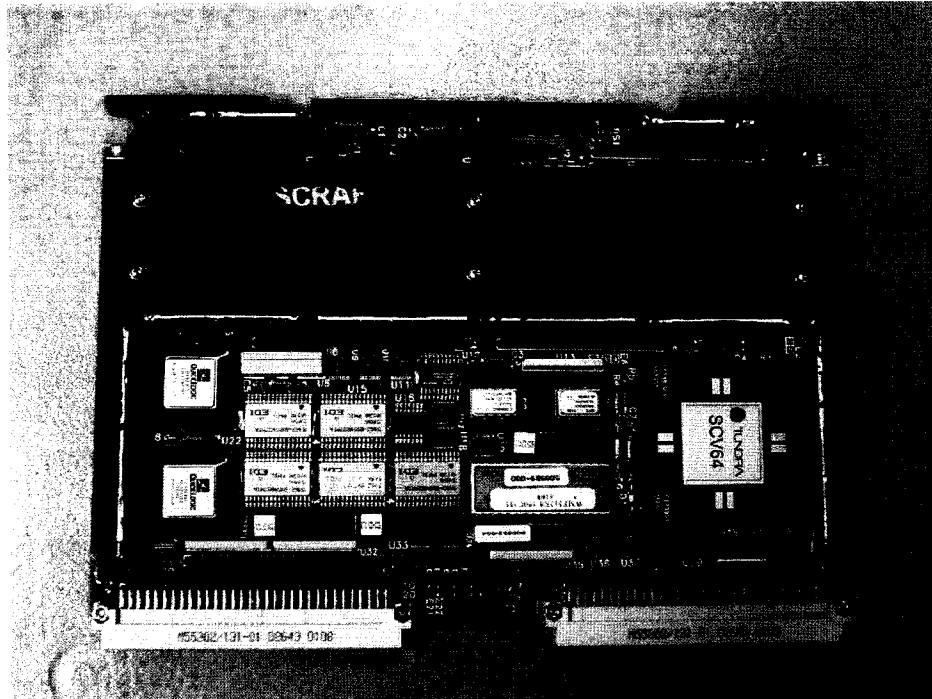


Figure 5: CCA Utilizing Combined PWB Core and External Frame Cooling Scheme (Component Side)

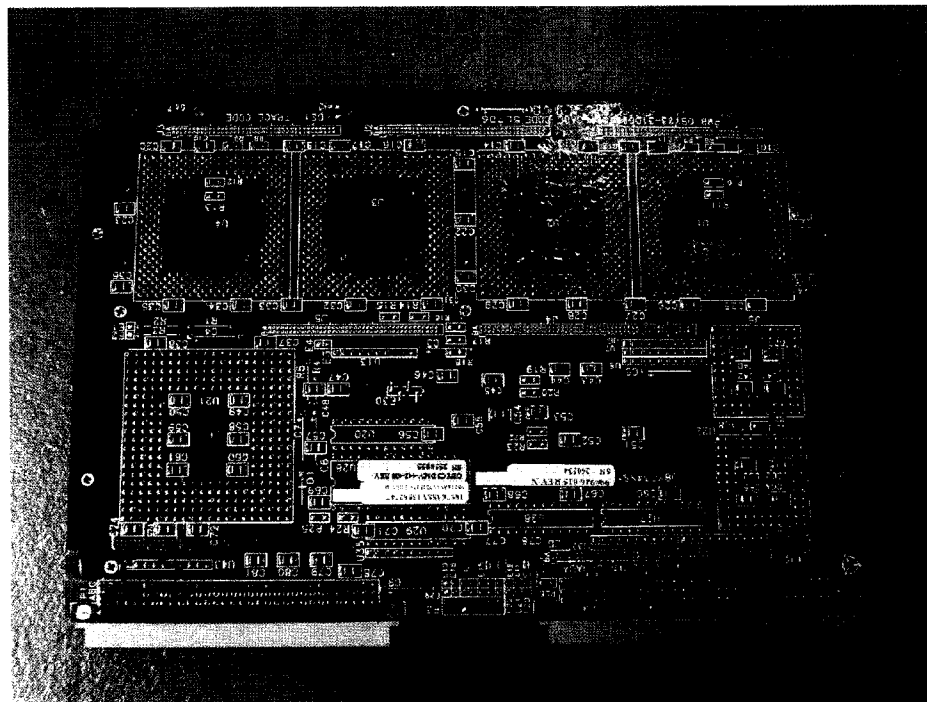


Figure 6: CCA Utilizing Combined PWB Core and External Frame Cooling Scheme (Solder Side)

This is necessary for several reasons. In addition to the sheer magnitude of the power dissipation of modern circuit cards, many processors and other high power devices dissipate too much power to rely on the thermal path from the active part of the device, the die, through the bottom of the device package to the PCB. A parallel heat path off the top of the device is necessary to dissipate the heat.

Even this design approach has limitations. Often circuit cards have limited spatial volumes, complex geometries, and mezzanine cards (removable modules which extend the functionality of the base circuit card, See Figure 7 and Figure 8), which limit the effectiveness of the metal cooling structure.

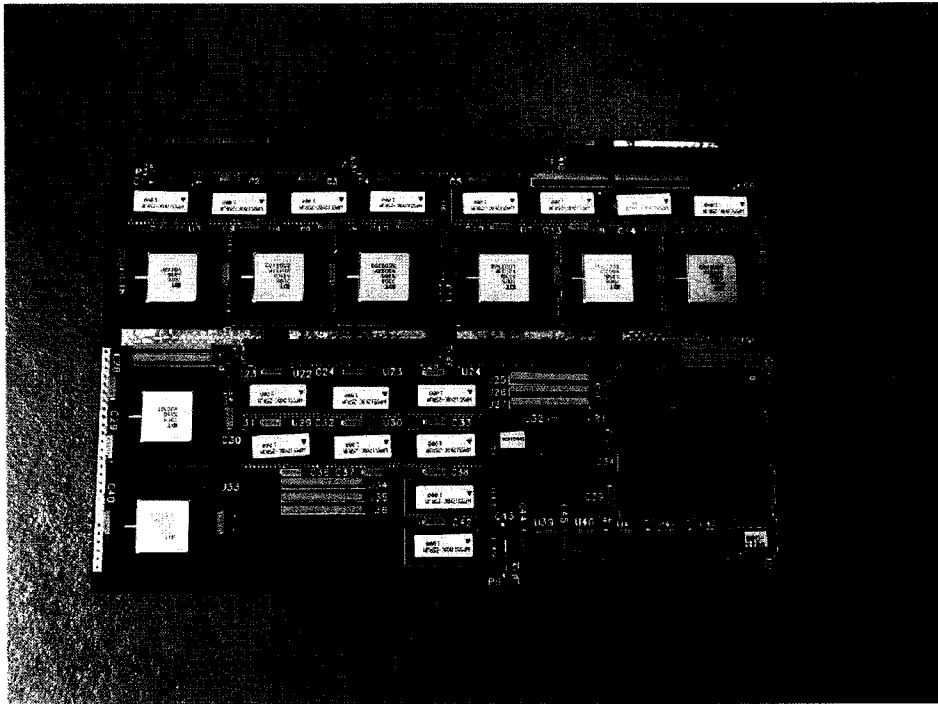


Figure 7: CCA Mezzanine Card used for Functionally Expansion (Component Side)

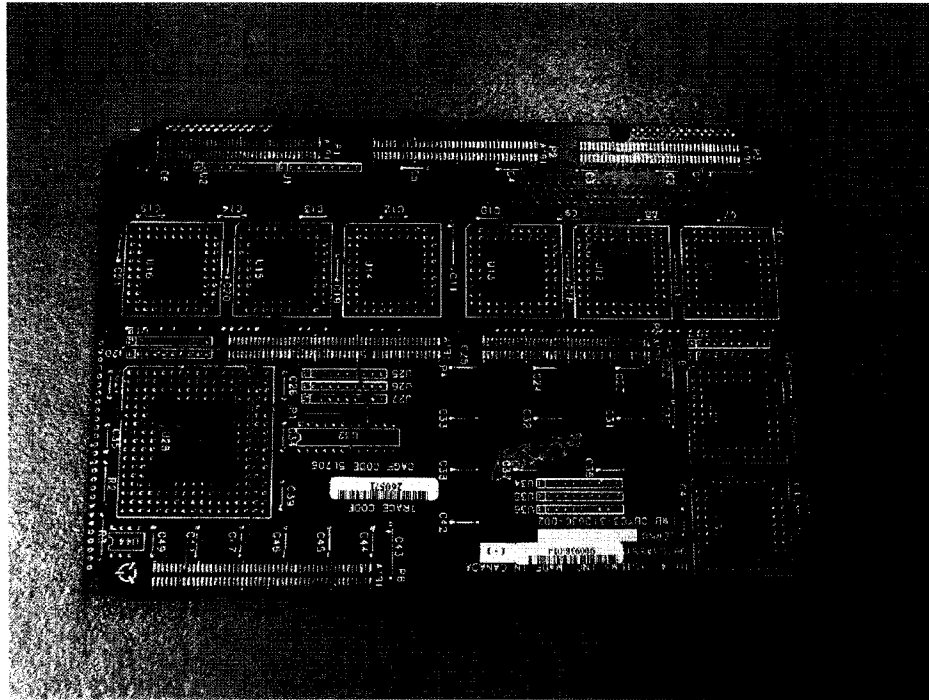


Figure 8: CCA Mezzanine Card used for Functionally Expansion (Solder Side)

Power dissipation is exceeding the heat transfer ability of common metals such as aluminum which has a thermal conductivity of approximately 180 – 200 W/m K. Therefore a means to extend the effectiveness of these structures is necessary. This study attempts to address this need through the investigation of Annealed Pyrolytic Graphite used in composite form with metal as a means to increase the effectiveness of these structures.

1.4 Objective

The objective of this study is to investigate the potential use of high thermal conductivity composite materials for electronics cooling applications paying particular attention to harsh environment applications such as those encountered in military use.

Specifically, this study will concentrate on the use of Annealed Pyrolytic Graphite (APG) embedded within a parent material such as aluminum, copper, or other metal.

1.5 Approach

The approach taken under this study is primarily analytical. A typical high power VME circuit card was chosen as a representative design. The first step was to analyze the aluminum structure, the frame, as an independent component. A Finite Element Model (FEM) was constructed which included volumes of APG embedded within the frame. This model was analyzed under a variety of conditions, material properties, configurations, etc. A prototype of this design was built and tested for comparison to the model. The results of these analyses and tests are presented herein.

2

Background

The ever-increasing power dissipation of electronics coupled with the shrinking availability and military grade devices and the military's desire to use cutting edge technology has fueled the demand for new and improved methods for electronics cooling. Military electronics in particular utilize conduction cooling in many applications due to its simplicity, ease of environmental protection, and in many cases superior thermal benefits. However, conduction cooling is being stretched to its limits and technologies to extend those limits are required. Using APG material to increase the effective thermal conductivity of cooling structures is a possible means to extend those limits.

2.1 Heat Transfer in Electronics Cooling

There are three fundamental modes of heat transfer, each of which is employed in the cooling of electronics depending on the application. Radiation heat transfer is most commonly used in the cooling of space electronics. Convection heat transfer, both natural and forced, is commonly used in commercial applications such as personal computers and consumer electronics, however some more sophisticated applications of convection heat transfer involve the use of liquid coolants for high heat flux applications. Conduction heat transfer is commonly used in military applications and is the mode of heat transfer examined by this study.

Conduction heat transfer takes place within a solid. When a temperature gradient is present within a solid material, thermal energy is transferred from the region of higher-temperature to the region of lower-temperature. The total rate of heat flow is proportional to the area normal to the heat flow path, the temperature gradient along that path, and the thermal conductivity of the material⁴, this is known as Fourier's law as illustrated in Equation 1:

$$\frac{dQ}{dt} = -kA \frac{dT}{dx}$$

Equation 1: Fourier's Law

In the electronics industry Fourier's law is used to model the heat flow within the materials associated with electronic components and assemblies. Heat is generated in the die of an electronics component and transferred by conduction through its lead-frame, substrate and over-molding towards the outer surfaces of the package. Upon reaching the outer surfaces of the package, the heat is transferred to the surroundings through conduction into the Printed Circuit Board or cooling structure such as a thermal frame, often through the use of thermal interface materials such as thermal adhesives, greases, pads, and phase change materials. The heat is then rejected from the electronics circuit card into a chassis which may use various forms of heat transfer to dissipate that heat to its surroundings.

Heat pipes, thermoelectrics, and high thermal conductivity composites are some of the potential technologies that can be used to improve heat transfer in electronic systems. This study concentrates on high thermal conductivity composites.

2.1.1 Isotropic Materials

In an isotropic solid structure conduction heat transfer is simply a function of the material geometry (cross sectional area, length of the conduction path), temperature gradient and thermal conductivity of the material. For conduction cooled electronics applications, one such structure is the metal frame often used as a primary or secondary thermal path as well as a stiffening member. The frame is typically manufactured of aluminum but can also be constructed of copper, beryllium, molybdenum or an alloy such as aluminum-beryllium or copper-molybdenum. Heat generated in active components conducts from the device die into the surrounding packaging material and through the package leads and surfaces into the PWB and surrounding structures. This heat may be transferred into the frame through contact with the PWB or through direct contact with the devices itself, usually through a thermal interface material.

Once heat has conducted into the frame it is transferred to the circuit card enclosure, the chassis, via direct contact at a clamped interface.

2.1.2 Laminates

Often, the primary heat transfer path in a conduction cooled circuit card design is the PWB itself. A PWB is a complex laminate structure comprised of multiple alternating conducting layers (usually copper) and insulating layers (often epoxy resin with fiberglass). These layers have vastly different thermal conductivity properties and geometries resulting in a complex and highly anisotropic heat transfer path. The PWB also contains copper plated vias that can be mechanically or laser drilled between two

layers, between several layers, or through the entire PWB affecting the thermal properties perpendicular to the laminate layers. The thermal conductivity of a PWB can be approximated using a weighted average calculation of the laminate materials and is dominated by the percentage of copper in the PWB. The thickness of copper is usually expressed in terms of ounces, i.e. 1 ounce of copper is approximately equivalent to a volume of copper that is 0.0014" thick and 1 ft², however, by convention 1 ounce of copper is assumed to be 0.0014" thick no matter what the area. Therefore, the equivalent thermal conductivity of a PWB laminate structure can be approximated by the expression:

$$K = \frac{t_l \cdot K_l}{t_{PWB}} + \frac{t_c \cdot K_c}{t_{PWB}}$$

Equation 2: Simplified Equivalent Thermal Conductivity of PWB Laminate Structure

Where;

t_l = The sum total thickness of the laminate material layers

K_l = The thermal conductivity of the laminate material

t_c = The sum total thickness of the copper layers

K_c = The thermal conductivity of the copper

In many cases, the laminate material contribution can be ignored since it is often several orders of magnitude smaller than the copper contribution to the effective thermal conductivity. This assumes that the copper content covers 100% of the area of the PWB and that the contribution of signal layer copper is ignored.

2.1.3 Heat Pipes

A heat pipe is a simple device that can quickly transfer heat from one point to another. It generally consists of a long sealed container or tube, usually aluminum or copper, whose inner surfaces have a capillary wicking material. The wick provides the capillary driving force to return the condensate to the evaporator. Different types of wicks and working fluids are used depending on the application for which the heat pipe is being used. Heat pipes are used in a wide range of applications like air-conditioners, refrigerators, heat exchangers, and electronics cooling.

Heat pipe have been used in laptop computers and space electronics for many years. Their unique ability to transport large amounts of heat from one point to another make them well suited for many niche applications. Heat pipes have not been used much in conduction cooled military applications due to questions around their ability to withstand the harsh environments encountered in these applications. Specifically, questions about the effect of shock and vibration on the capillary action of a heat pipe were raised. A study by Chad St. Louis⁵ addressed these questions in his Master's Thesis. The results of this study indicate that g-forces have little effect on the capillary limit of most heat pipes. Therefore, heat pipes can play a role in certain conduction-cooled electronics applications where the transport of heat from one location to another is crucial; however, this technology is somewhat limited due to geometrical considerations and is often a single design specific solution.

2.1.4 Composites

Composite material can be defined as two or more materials bonded together⁶. Composites have been used in electronics applications for many years, for example, PWBs are essentially glass-fiber reinforced polymers which belong to a class of composites called Polymer Matrix Composites (PMC). In addition, Copper-Invar-Copper (Cu-I-Cu) and Copper-Molybdenum-Copper (Cu-Mo-Cu) are two examples of materials employed by the industry which belong to a class of composites called Metal Matrix Composites (MMC). Two other classes of composites include, Ceramic Matrix Composites (CMC) and Carbon/Carbon Composites (CCC).

Many of the composite materials used in the electronics industry today offer advantages for structural considerations such as density, stiffness, and Co-efficient of Thermal Expansion (CTE). Low-density composites are desirable for space electronics where weight costs are high. Stiff materials are advantageous in applications with high vibration requirements while materials with low CTE are often bonded to or between PWBs to match components such as ceramic BGAs or direct attach silicon die.

For thermal applications composites have been used to create high conductivity structures such as heat sinks and thermal cores from such elements as diamond particles, graphite flakes and carbon fibers. This study will focus on one such composite, Annealed Pyrolytic Graphite

3 Annealed Pyrolytic Graphite

3.1 Introduction to Annealed Pyrolytic Graphite

Pyrolytic Graphite (PG) is defined as a material with a high degree of preferred crystalline orientation of the C-axes perpendicular to the surface of the substrate, obtained by graphitization heat treatment of pyrolytic carbon or by chemical vapor deposition at temperatures above 2500 K. Hot working of pyrolytic graphite by heat treatment under compressive stress at temperatures above 3000 K results in Annealed Pyrolytic Graphite (APG). APG is defined as a pyrolytic graphite with an mosaic spread angle of less than 1 degree when measured by X-ray diffraction⁷. Simply put, APG consists of many atomic layers of carbon atoms, which are “highly oriented” between each other.

APG is used for a variety of applications in scientific research including sputtering targets, ion beam grids, crucibles for ultra high vacuum, and substrate materials for scanning tunneling microscopy. Its unique properties such as high purity, chemical inertness, impermeability, directional electrical and thermal characteristics, low etch rate, and self-lubrication make it a desirable material to scientists. For example, it provides an excellent substrate for elemental analysis due to its purity, since it is comprised entirely of carbon. Its extremely smooth surface provides a featureless

background except at atomic level resolution where its structure shows the hexagonal rings characteristic of graphite.

The modern-day material known as Annealed Pyrolytic Graphite (APG) originated from a material that was once called Kish graphite, a by product of the steel making process which resulted during the cooling of molten steel. Early researchers used Kish graphite for producing spectrometer crystals and atomically smooth surfaces. However, Kish graphite was limited in this application due to impurities and relatively small size (4 to 5 mm in diameter)⁸.

It is the thermal properties of APG that generate the greatest interest relative to this study. Being a highly structured carbon based material, the thermal conductivity of this material is very high relative to metals and other materials commonly used in electronics applications.

3.2 Physical properties

APG is an anisotropic material with a reported thermal conductivity in the range of 400 – 3000 W/m K in the X-Y plane, and 10 – 25 W/m K in the Z direction^{9,10}. It has a specific gravity of 2.3 compared to 2.7 for aluminum. The coefficient of thermal expansion (CTE) is –1 ppm/K in the X-Y plane and 25 in the Z direction¹¹. Being a layered structure, APG cleaves similarly to mica or shale. The material itself is weak and brittle and nearly always requires the use of an encapsulating material to provide the necessary mechanical properties for practical applications. Encapsulating materials

often used are aluminum, copper, graphite fibre/polymer, Polyimide and others. These materials dominate the structural properties of the composite.

3.3 Industry Experience

There are currently several companies supplying Pyrolytic Graphite or products derived from PG for use in a variety of industries and applications. For scientific purposes companies such as GE Advanced Ceramics and Structure Probe Inc. supply research grade PG and products such as crucibles, tubes and coatings. GE Advanced Ceramics as well as companies such as Panasonic Industrial Solutions, Ceramics Process Systems Corporation and k-Technology Corporation supply standard and custom designed products that are targeted toward heat transfer applications.

GE Advanced Ceramics supplies APG encapsulated in Aluminum, Copper and Graphite/Polymer in custom sizes. These composites are generally supplied as a simple sheet for use as heat spreaders, as the base of heat sinks or as thermal cores laminated to or between PWBs.

Panasonic Industrial Solutions supplies PG sheet material with a variety of backing materials pre-attached such as Silicon layered tape, Polyimide tape and conductive adhesive tape. These sheets are very thin, 0.1mm, and are used in a variety of electronics applications such as mobile phones, laptop computers, semiconductor processing equipment and optical communications equipment.

Ceramics Process Systems (CPS) Corporation supply custom manufactured encapsulated APG components for a variety of electronics cooling applications. CPS

main area of expertise lies in the use of Aluminum Silicon Carbide (AlSiC) material in a net-shape cast manufacturing process. The AlSiC encapsulating material offers an advantage of Aluminum alloys from a CTE perspective. AlSiC has a CTE in the range of 8.7 to 11.7 ppm/°C which more closely matches the CTE of materials often used in electronics applications versus 23.8 ppm/°C for most Aluminum alloys¹². However, the casting process introduces some disadvantages in terms of design and cost. The casting must be designed such that it easily releases from the mold, it is somewhat difficult to attain tight tolerances and there is a large investment required for each mold making small volume manufacturing impractical and expensive.

k-Technology Corporation designs and manufactures products for electronics cooling applications using APG encapsulated in a variety of parent materials. Common parent materials include Copper, Aluminum and Cu-Mo-Cu. The process used to encapsulate the APG within the parent material is generally Hot Isostatic Pressing (HIP).

4 Thermal Analysis

This chapter describes the thermal analysis approach taken and results obtained to determine the thermal performance of a composite material conduction frame consisting of aluminum and APG material. The analysis was performed using a model of an actual thermal frame and analyzed with a variety of geometrical, material, and design parameters as a sensitivity analysis.

4.1 Background

There is a wide variety of custom and standard electronics module formats used in the electronics industry. The products that CWCEC produces are primarily based on the VME standard in both an air-cooled and conduction-cooled format. The physical formats are defined in IEEE standards 1101.10 for air-cooled and 1101-2 for conduction-cooled modules. Electronics modules can provide a variety of functions such as Digital Signal Processing (DSP), graphics or general purpose Single Board Computers (SBC). Many current designs of these modules make use expansion daughter cards that expand the functionality of the module. The most common form of expansion module used in the VME industry is a PMC module. The cooling of the base card module presents its own challenges which are exaggerated when the requirement for expansion modules is included. The

Finite Element Model analyzed in this study consists of a thermal frame designed to address both the base module and PMC module cooling requirements.

4.2 Frame Finite Element Model

A three dimensional model of a typical thermal frame was constructed using Pro/Engineer solid modeling software. The use of Pro/Engineer allowed quick changes to be made to the model geometry and facilitated the construction of assembly models comprised of multiple individual parts. Pro/Mechanica™ finite element analysis software was used to discretize the model and perform all analysis. While Pro/Mechanica™ is a somewhat simplified FEA tool it allows for complex geometries to be modeled and analyzed with relative ease due to its use of high order elements.

The thermal frame model was constructed as a one piece solid and then hollows were cut into the frame in which separate piece parts could be inserted representing the APG inserts. Thus, the geometric model was an assembly of several individual piece parts. By varying material properties, loads and geometrical parameters a design study was conducted to determine results for a variety of scenarios. Figure 9 and Figure 10 illustrate the features of the FEM including APG insert locations, boundary conditions and heat loads. Note, the aluminum is in blue and the APG in grey, however the mid-section APG is shown exposed (aluminum skins removed).

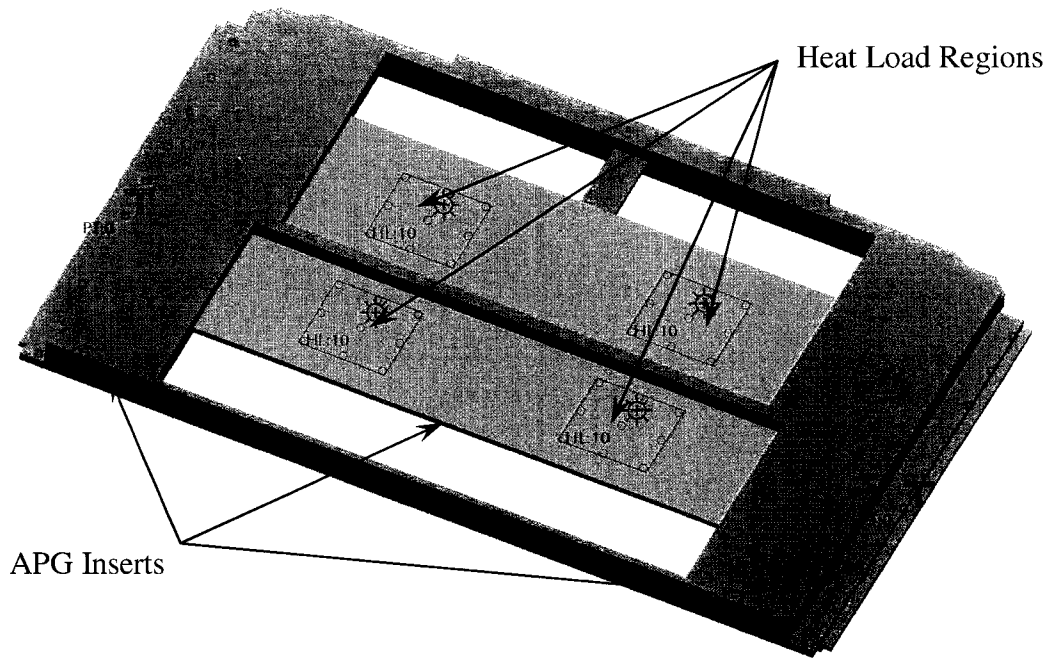


Figure 9: Top View of Finite Element Model

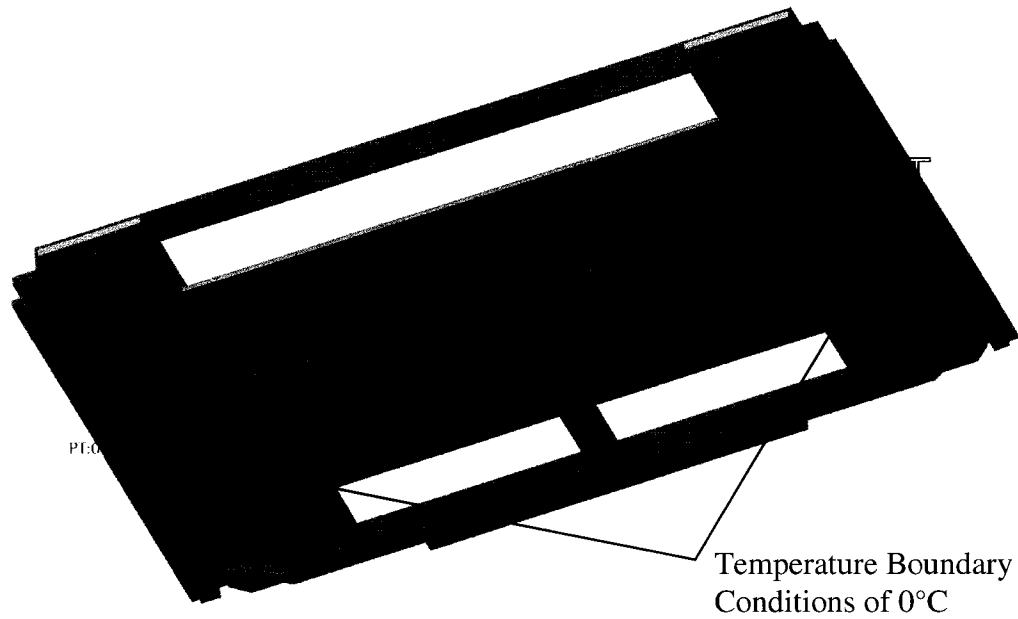


Figure 10: Bottom View of Finite Element Model

The purpose of analyzing the frame independent of the rest of the components of the circuit card assembly was to optimize several of the relevant design and

material parameters and determine the sensitivity of the model to variations in some of these parameters.

4.2.1 Geometry/Boundary Conditions/Heat Loads

The Finite Element Model represents a typical thermal frame used on a VME circuit card assembly employing 4 processors and various other integrated circuits. This design represents a digital signal processing CCA, one of the most thermally challenging designs currently implemented by CWCEC. This design facilitates the use of two single widths or one double width conduction-cooled PCI Mezzanine Card (PMC) card designed per ANSI/VITA 20 specification.

To simplify the analysis, all holes, fillets, chamfers and detail features were removed from the solid model; however, the overall shape, dimensions, and features are representative of the actual design.

Heat loads were applied in four regions near the center of the frame. Their location, size and flux density are representative of the size and proposed location for heating elements that will be used during thermal testing of the prototype frames.

4.2.2 Material Properties

The standard thermal frame is manufactured of aluminum alloy 6061 and thus the material properties of this alloy were used as the basis for the parent material of the composite thermal frame. The thermal conductivity is assumed to be 180

W/m K. The material is assumed to be isotropic, i.e. having the same thermal conductivity in all three directions.

As discussed previously the material properties of the APG are highly dependant upon the quality of the material in terms of crystalline orientation and the refining process. A baseline thermal conductivity of 1530 W/m K is used in the in-plane directions of the material while an orthogonal thermal conductivity of 10 W/m K is assumed. The supplier of the material and components, k-Technology, has each piece of material measured for thermal conductivity by an independent party third party using a flash diffusivity method¹³. This ensures that each piece of APG used has a thermal conductivity of 1530 W/m K or greater at room temperature. Figure 11 illustrates the temperature dependence of the APG material thermal conductivity as measured on two representative samples, courtesy of k-Technology.

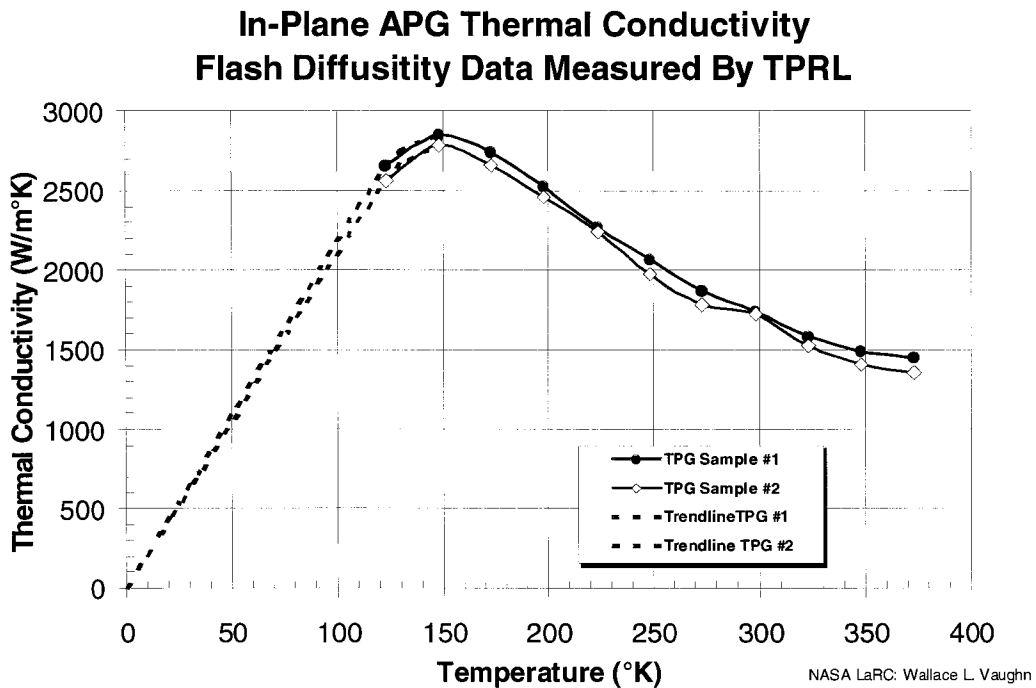


Figure 11: In-plane APG Thermal Conductivity

As illustrated above the typical measured thermal conductivity of the APG is approximately 1700 W/m K at 300 K (near room temperature). At 375 K the thermal conductivity of the material is approximately 1300 W/m K or greater. The maximum anticipated use temperature for the thermal frame is approximately 375 K (~100 °C) since the temperatures of the integrated circuits being cooled by the frame are often limited to temperatures in the range of 100 - 125 °C.

Throughout the process of analyzing the thermal frame with and without APG inserts, whenever the model was analyzed as aluminum only the material volume representing the APG inserts were left in place and the thermal conductivity of aluminum was assigned to those volumes. This allowed for the reuse of the finite

element mesh structure for a variety of analysis cases with and without PG and forced a finer mesh in those areas.

4.2.3 Design studies/Sensitivity Analysis

The thermal analysis was performed for a variety of geometrical, material and heat load conditions. The sensitivity of the results to the thermal conductivity of the APG in both the in-plane and through-plane directions was analyzed. The thickness of the APG inserts was varied and the effect of inserting APG in various combinations of locations within the frame structure was also explored.

With a thermal conductivity that varies over temperature and according to manufacturing parameters, it is important to understand the impact of using a APG composite frame in rugged electronics cooling applications where ambient temperature can vary dramatically. For the purpose of this study the typical thermal conductivity of APG was assumed to be 1530 W/m K. To determine the sensitivity of the results to variation in thermal conductivity, resulting from an operational temperature of approximately 100°C, the analysis was performed at 1200 W/m K.

Due to the highly anisotropic nature of the APG material, the specific heat transfer rate in the through-plane direction of the material will be significantly different than that in the in-plane directions. Generally, the APG inserts will be thin relative to their length, this is due to the nature of the circuit card design and the need to occupy as little volume and have the minimum mass possible.

Therefore, the material will be oriented such that the in-plane directions will be long relative to the through-plane. The effect of the low through-plane thermal conductivity on the results is modeled using a thermal conductivity of 10 W/m K as a low value and 20 W/m K as a high value.

As previously mentioned, the APG inserts will be thin and long and as such the thermal resistance, which is proportional to cross-sectional area, will be highly dependant upon the thickness of the material. The analysis was conducted using two different thicknesses of APG in the central portion of the thermal frame where length was greatest and thickness was least. The APG thickness was not varied in the other areas of the frame where a greater overall thickness could be easily achieved.

The thermal frame chosen for this study is representative of a typical design utilizing multiple processors and mezzanine cards. In order to facilitate these features, the frame design has regions at different relative elevations that can accommodate different sections of APG material. The effect of including APG in different combinations of these regions was examined.

4.2.4 Assumptions

Finite element analysis is an idealization of a real situation with many simplifying assumptions. The goal is to minimize those assumptions and/or the impact of those assumptions on the results of the analysis such that the results are as realistic as possible. The objective of this study is to provide a comparative

thermal analysis between an all aluminum thermal frame with an aluminum/APG composite thermal frame. Therefore, the absolute results are not as critical as the relative results. The following assumptions apply to the finite element analyses of the thermal frame models.

1. **No interface resistance at the APG/aluminum boundary.** It is assumed that the interface between the APG inserts and the aluminum parent material is a perfect one at which no interface resistance exists. The manufacturing process, discussed in section 5, results in a very good surface to surface joint with minimal thermal resistance. As a sanity check, an interface resistance with assumed characteristics can be calculated as follows:

$$\text{Area (A)} = 0.03 \text{ m} \times 0.1 \text{ m} = 0.03 \text{ m}^2$$

$$\text{Length (L)} = 0.00001 \text{ m (0.01mm)}$$

$$\text{Thermal conductivity of air @ 375 K (k)} = 0.03 \text{ W/m K}$$

$$\text{Therefore, thermal resistance} = L/k \cdot A = 0.011 \text{ }^\circ\text{C/W}$$

2. **Simplified geometry.** For the purpose of simplifying the FEM all holes and fillets were removed from the original frame design. The model was de-featured to decrease mesh size and facilitate faster solve times. For comparison purposes all models were geometrically identical.

3. **Conduction only.** In all cases conduction heat transfer was the only mode of heat transfer considered.
4. **Ideal boundary conditions.** In all cases a uniform temperature boundary condition was applied to an area of the frame representing the interface to the cold wall (chassis).
5. **Uniform heat flux.** In all cases four regions were defined on the surface of the frame representing four areas of heat flux, each was modeled as a uniform heat flux.
6. **40 W total heat flux.** The heat flux applied to each of the four surface regions was 10 W for a total of 40 W. This value was chosen since it represents the approximate maximum power dissipation of resistive heating elements chosen for test purposes. This allows for direct comparison of analytical and empirical results.
7. **APG in-plane thermal conductivity.** As discussed on section 4.2.2 the minimum in-plane thermal conductivity of APG is 1530 W/m K at room ambient temperature according to the material supplier. The temperature dependant nature of this property results in a lower thermal conductivity at its anticipated use temperature of 100 °C. Using the curve presented in Figure 11 the estimated thermal conductivity of APG at 100°C is 1200 w/m K.

8. **APG through-plane thermal conductivity.** The reported through-plane thermal conductivity of APG is approximately 15 W/m K. The thermal conductivity was conservatively assumed to be 10 w/m K and optimistically assumed to be 20 W/m K for the purposes of performing sensitivity analysis. For thin sections of APG this assumption is less critical but as sections become thicker it is more important to model this material property accurately.

9. **Constant APG material properties.** For simplicity of analysis it was assumed that the material properties of the APG do not vary throughout its volume as temperature differentials developed. I.e. with one end of the material at a different temperature from the other end the material properties would vary along its length and affect the overall results slightly. Since the maximum temperature differential expected is on the order of 20 °C or less, this variation in thermal conductivity would be on the order of 75 to 100 W/m K over the anticipated use temperature range.

4.2.5 Results

The following sub-sections discuss the results of the finite element analysis in terms of the various factors considered for variation.

4.2.5.1 APG Location

The baseline analysis, case 1, upon which all other analysis will be compared to is a standard aluminum thermal frame with no APG inserts representing current conduction cooling technology. The frame was modeled as an assembly of several piece parts representative of the APG inserts and aluminum encapsulating material but all pieces were assigned the thermal conductivity of aluminum. The total heat flux applied to the model was 40 W (4 x 10 W). Figure 12 illustrates the results of analysis case 1 with a maximum temperature of 34.88 °C.

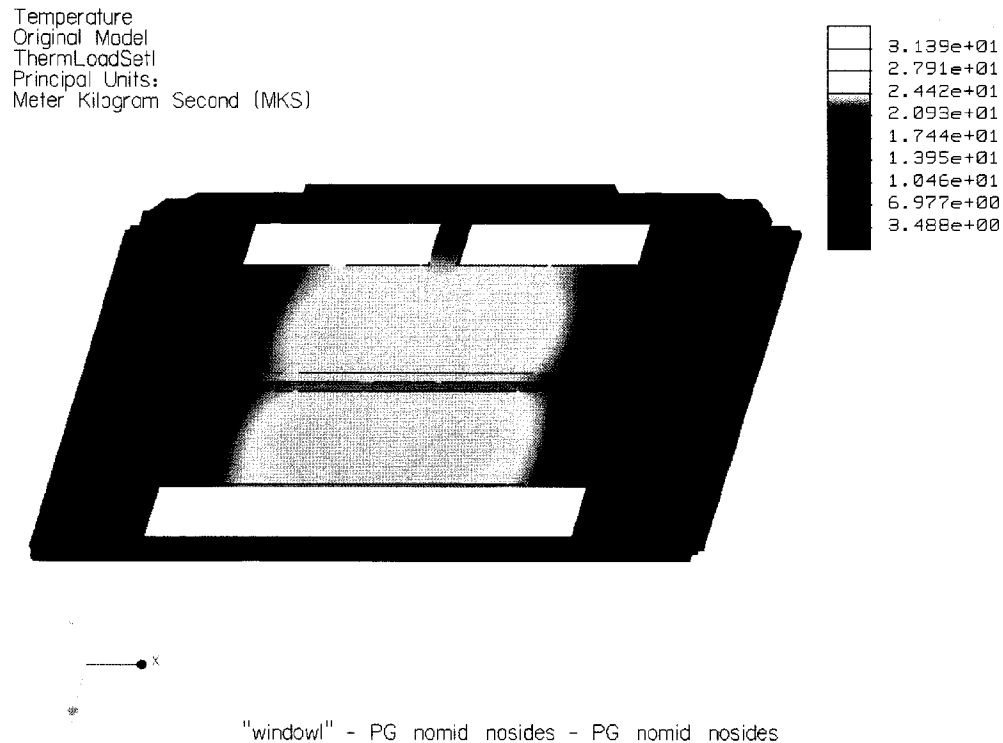


Figure 12: FEA Results of Analysis Case 1, All Aluminum Frame, 40 W.

The maximum temperature occurs near the center of the frame in the regions of the applied heat flux as illustrated by the white regions on the isothermal plot.

Case 2 is a composite frame with APG inserts included in both the mid-section and side-sections of the frame. Figure 13 illustrates the results of analysis case 2 with a maximum temperature of 14.92 °C.

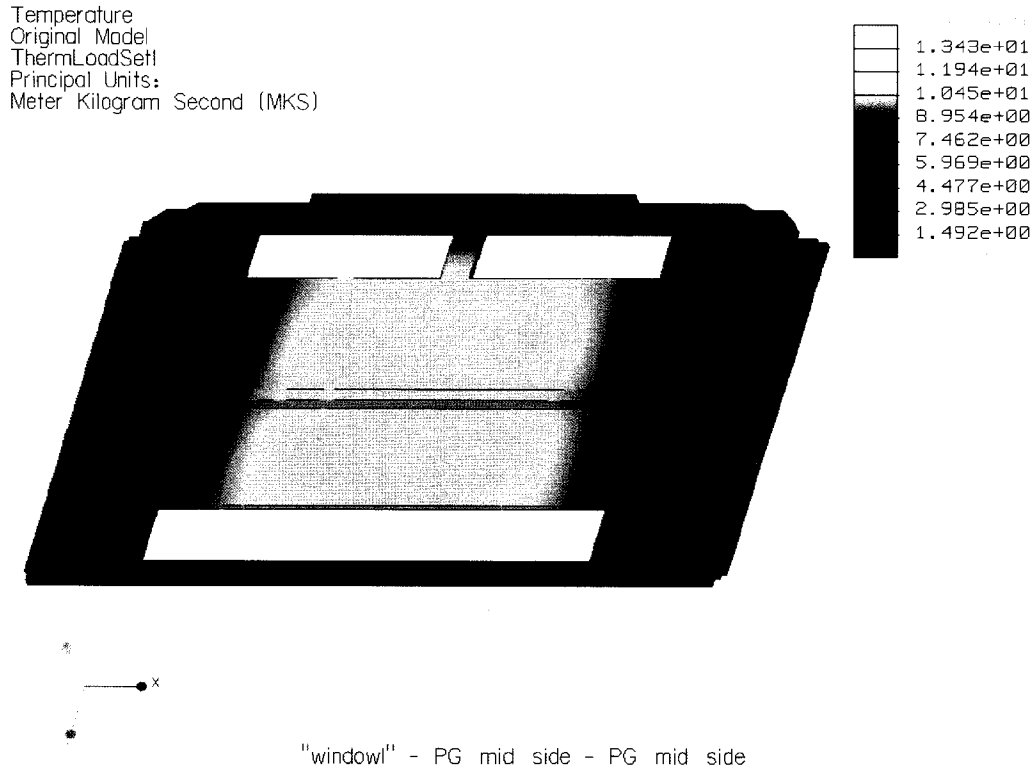


Figure 13: FEA Results of Analysis Case 2, APG Mid and Side Sections, 40 W.

Case 3 is a composite frame with an APG insert included in the mid-section and aluminum included in the side-sections. Figure 14 illustrates the results of analysis case 3 with a maximum temperature of 17.51 °C.

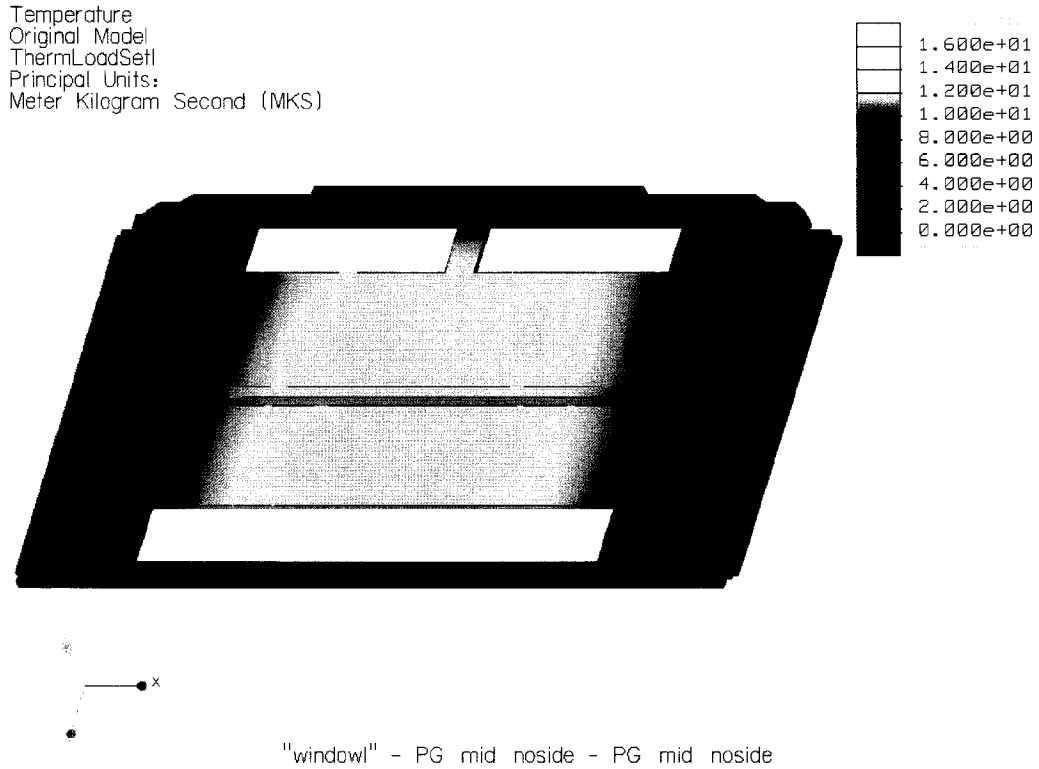


Figure 14: FEA Results of Analysis Case 3, APG Mid-Section, 40 W.

Case 4 is a composite frame with APG inserts included in the side-sections only and aluminum included in the mid-section. Figure 15 illustrates the results of analysis case 4 with a maximum temperature of 32.19 °C.

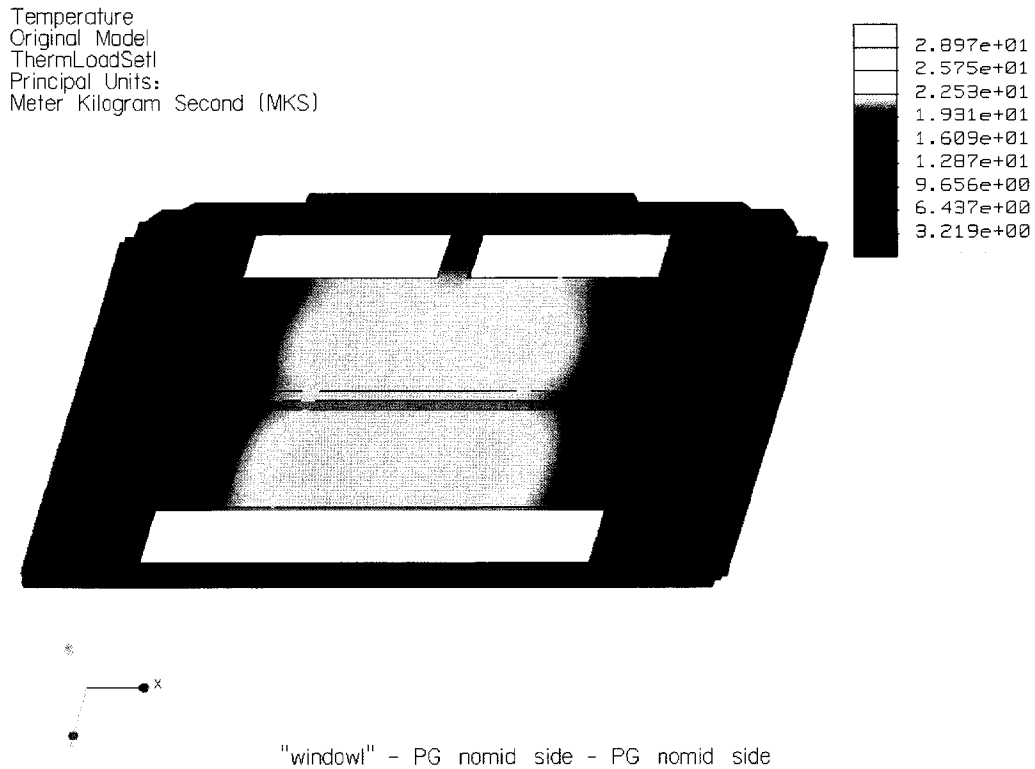


Figure 15: FEA Results of Analysis Case 4, APG Side-Sections, 40 W.

4.2.5.2 APG Orthogonal Thermal Conductivity

The highly anisotropic nature of the APG results in a thermal conductivity in the through-plane direction that is in the range of 10 – 20 W/m K. For the majority of the finite element analysis cases the thermal conductivity value used was 10 W/m K. As a check, the thermal conductivity was changed to 20 W/m K to determine the sensitivity of the model to this parameter.

Case 5 is a composite frame with APG inserts included in both the mid-section and side-sections of the frame. Figure 16 illustrates the results of analysis case 5 with a maximum temperature of 14.22 °C.

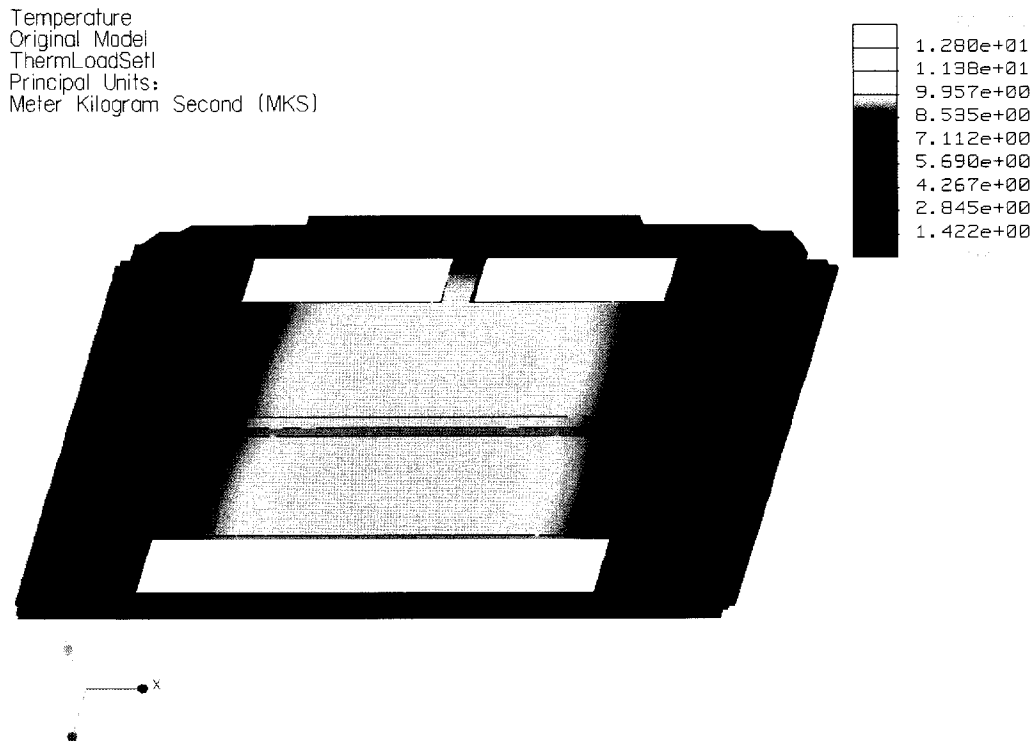


Figure 16: FEA Results of Analysis Case 5, APG, 20 W/m K Thru-Plane, 40 W.

4.2.5.3 APG Thickness

The thermal resistance of a material is directly proportional to its thickness perpendicular to the direction of heat flow. The thicknesses of the APG inserts were predefined by k-Technology to be 0.023” in the mid-section and 0.080” in the side-sections to meet manufacturability requirements. In order to determine the sensitivity of the model to the thickness of the APG, the model was modified

to allow for 0.040” APG in the mid-section. The side sections kept at their original thickness.

Case 6 is a composite frame with APG inserts included in both the mid-section and side-sections of the frame. Figure 17 illustrates the results of analysis case 6 with a maximum temperature of 11.49 °C.

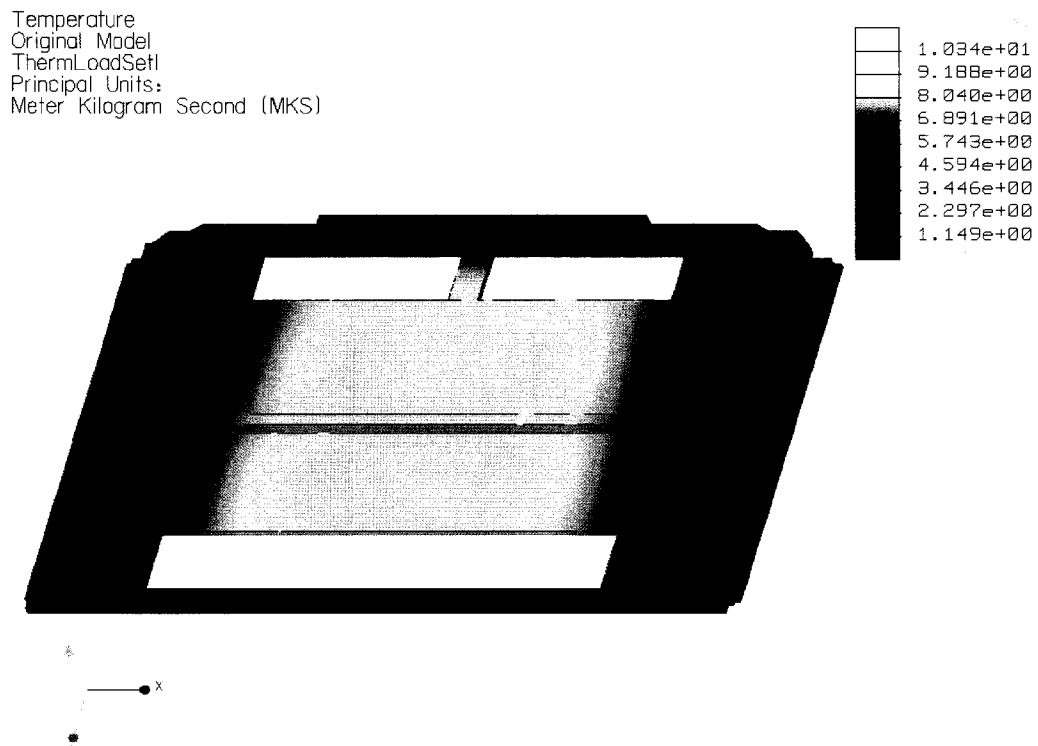


Figure 17: FEA Results of Analysis Case 6, 0.040” Thick APG, 40 W.

4.2.5.4 APG In-plane Thermal Conductivity

Although the minimum thermal conductivity of the APG material is specified by the supplier, k-Technology, to be 1530 W/m K or greater at room temperature it is important to understand the impact of varying thermal conductivity on the results

important to understand the impact of varying thermal conductivity on the results of the thermal analysis. One case of the model was run with an in-plane thermal conductivity of 1200 W/m K for the APG inserts. Note, for this case the APG thickness in the mid-section was 0.040" similar to case 6.

Case 7 is a composite frame with APG inserts included in both the mid-section and side-sections of the frame. Figure 18 illustrates the results of analysis case 7 with a maximum temperature of 12.86 °C.

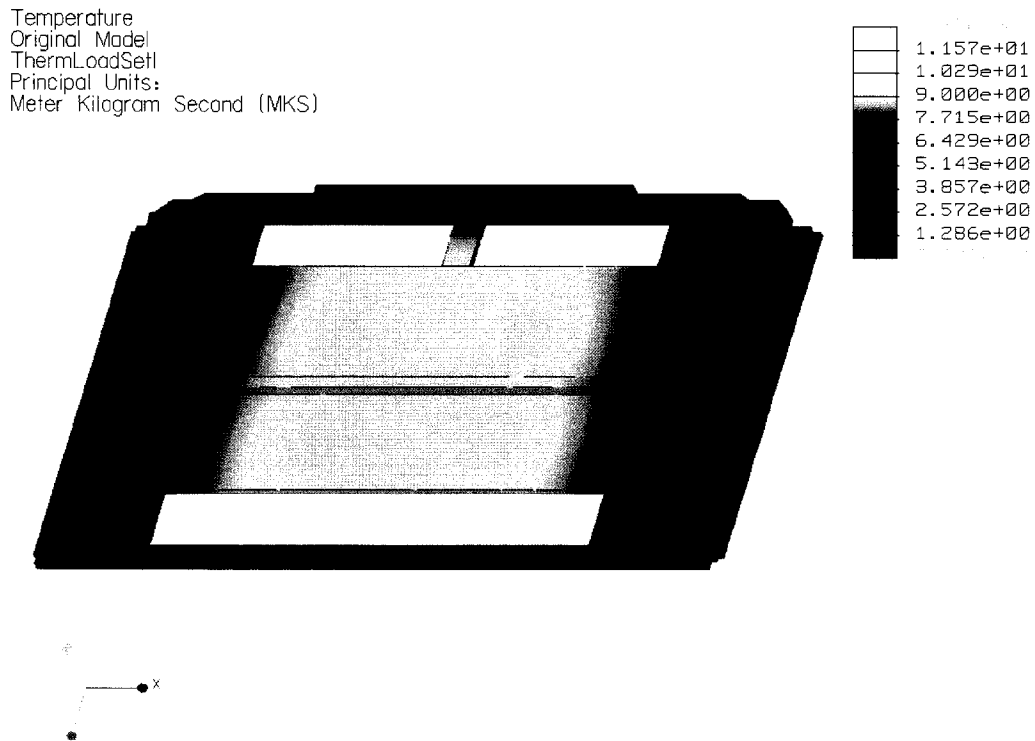


Figure 18: FEA Results of Analysis Case 7, 0.040" Thick APG, 1200 W/m K, 40 W.

Case	APG Location	APG In-Plane Conductivity (W/m K)	APG Thru-Plane Conductivity (W/m K)	APG Mid-Section Thickness (inches)	Results - Maximum Temperature (°C)
1	NA - Aluminum Only	NA	NA	NA	34.88
2	Mid Section and Side Sections	1530	10	0.023	14.92
3	Mid Section	1530	10	0.023	17.51
4	Side Sections	1530	10	0.023	32.19
5	Mid Section and Side Sections	1530	20	0.023	14.22
6	Mid Section and Side Sections	1530	10	0.040	11.49
7	Mid Section and Side Sections	1200	10	0.040	12.86

Table 1: Summary of Finite element Results

The baseline finite element analysis of the all aluminum thermal frame indicates that the maximum temperature of 34.88 °C occurs near the center of the frame in the regions of the applied heat flux. With APG inserts embedded within the aluminum in both the mid-section and side-sections of the frame the maximum

temperature is reduced to 14.92 °C representing a decrease of 57% over the baseline case. When the APG inserts are included in the mid-section of the frame and excluded from the side sections the maximum temperature increases to 17.51 °C. This represents a decrease of 50% over the baseline case. When APG inserts are included in the side-sections of the frame and excluded from the mid-section the maximum temperature increases further to 32.19 °C. This represents a decrease of 8% over the baseline case. These results indicate that the mid-section APG insert dominates the overall reduction of temperature for this particular design.

The out of plane thermal conductivity of the APG is in the range of 10 – 20 W/m K, approximately two orders of magnitude lower than the in-plane thermal conductivity. The results of the analysis indicate that for a limited range of values there is very little effect on the overall results of the finite element analysis. Using a realistically high thermal conductivity of 20 W/m K the maximum temperature was determined to be 14.22 °C representing a decrease of less than 1% over the baseline case using a thermal conductivity of 10 W/m K.

The allowable thickness of the APG is governed by the design, geometry and manufacturability of the thermal frame design. The baseline APG model utilized inserts of 0.023” thickness in the mid-section and 0.080” in the side-sections. An analysis of the frame model using a thicker mid-section APG insert of 0.040” resulted in a maximum temperature of 11.49°C. This represents a decrease of 67% over the baseline aluminum case and 23% over the 0.023” thickness case.

The in-plane thermal conductivity of the APG is highly temperature and process dependant. The minimum in-plane thermal conductivity specified by k-Technology is 1530 W/m K at room temperature; this value was used for the baseline APG case. The thermal conductivity was reduced to 1200 W/m K and the analysis resulted in a maximum temperature of 12.86 °C. This represents a decrease of 11% when compared to the 0.040" thick mid-section APG case. The in-plane thermal conductivity of the APG is the most critical parameter in determining the overall thermal performance of the cooling frame. Since the frame is a composite of two materials the effective thermal performance does not vary linearly with the thermal conductivity of the APG inserts. This is discussed in further detail later in this document.

5 Fabrication

This chapter briefly discusses the manufacturing processes involved in the fabrication of an Aluminum/APG composite piece part. Process limitations and design guidelines are examined which restrict the implementation of this technology.

5.1 General Fabrication Method

The fabrication of a completed Aluminum/APG composite piece part involves the utilization of several different manufacturing techniques and technologies. The process begins with the manufacturing of the APG inserts which are embedded with the parent metal using the Hot Isostatic Pressing (HIP) method. The roughly formed composite is usually post-machined to its final shape and detail using Computer Numerically Control (CNC) machining processes and the final piece part can then be surfaced treated to prevent corrosion and provide the desired surface finish. This process is discussed in greater detail in the following paragraphs.

The APG material is obtained by either heat treatment of pyrolytic carbon or chemical vapour deposition at temperatures above 2500 K and then further hot working to temperatures above 3000 K. Due to the planer nature of the material, smaller sections are cleaved from a larger piece to obtain the desired size and

thickness. The APG insert is prepared by shaping, cutting and pre-drilling. For example, any holes that are to be present in the final composite design must first be predrilled in the APG such that the parent metal material can fill the voids and receive the drilled holes. It is undesirable to drill or cut through the finished composite piece part exposing the APG since the APG is brittle, susceptible to damage from certain metal surface treatment process, such as anodizing, and may release electrically conductive particles which could be detrimental to electronics assemblies.

Once the APG inserts has been prepared it is embedded in the parent metal material using the HIP process. In this process, metal powder is formed into a mold, usually made of steel, and out-gassed, the APG is inserted in the desired locations and the combination is placed in a furnace under simultaneous application of high pressure (on the order of 100 MPa) and a temperature of approximately 1100 °C for several hours¹⁴.

It is desirable to form the composite as close to the final shape as possible to minimize post machining, however for complex parts it is difficult to avoid this step. Final details, tapped holes, tight tolerance and other features are added through the CNC machining process.

The final step in producing a finished piece part is surface treatment. Generally, most metals require a surface treatment to prevent corrosion and oxidation, add surface electrical insulation, or provide a desired aesthetic look. Examples of common surface finishes include zinc plating, nickel plating, and anodizing.

5.2 Fabrication Issues

There are limitations to the process described in Section 5.1 which restrict the design flexibility of the Aluminum/APG composite. Some of these issues include tolerancing, locating the APG within the parent material, size limitations of the APG (area, thickness), and flexing.

The nature of the HIP process results in difficulty controlling the location of the APG inserts precisely. Placing the APG inserts becomes critical when trying to achieve thin sections or tight tolerances in the final design. For electronics cooling applications, thin sections are desirable so as to not occupy too much volume normally used for integrated circuit components in certain electronics form factors such as VME.

The locations of multiple APG inserts within a single composite piece part, such as the sample frame manufactured under this study, present difficulty when these sections are placed on different horizontal planes or if they are in different orientations, for example if high thermal conductivity is required in two directions.

The manufacturing of the APG material itself is a relatively expensive process and large geometries are difficult to achieve, therefore the size and thickness of the APG inserts drive the design of the composite. It is preferred to maintain thin sections of the APG since its thermal conductivity is poor in the through-plane direction.

Due to the brittle nature of the APG material, exaggerated flexing of the composite piece part may result in damage and degradation in thermal performance. Therefore, if a design is to be subjected to high bending stresses, it should be tested prior to and after life-cycle testing to determine if the composite retains its desired mechanical properties.

6 Experimental Test

This chapter describes the experimental testing undertaken to measure the thermal performance of the composite frame in comparison to the all aluminum frame. Testing was performed over a range of power dissipations and ambient temperatures to establish trends in the data and determine the susceptibility of the thermal conductivity of the APG material to temperature. Additionally, an effort was made to correlate the actual measured performance of the frames to the finite element analysis presented earlier in this document.

6.1 Thermal Frame Testing

Thermal testing is performed to determine the actual performance of the composite thermal frame in comparison to the all-aluminum version. The following sections describe the test specimens, set-up, procedure and results of the thermal testing.

6.1.1 Test Specimens

The test specimens were physically representative of the frame design analyzed previously in this document. The all aluminum version is CWCEC part number 221513-000 (Revision -) and is shown in Figure 19, the composite version was based on this part number but had some detailed features removed for ease and speed of prototype manufacturing. Figure 20 shows the composite thermal frame with the mid-section APG

inserts partially visible while Figure 21 shows a cross sectioned view with the different thickness APG inserts visible. Note that the all aluminum frame has a black anodize surface finish treatment while the composite frame has a raw untreated aluminum finish.

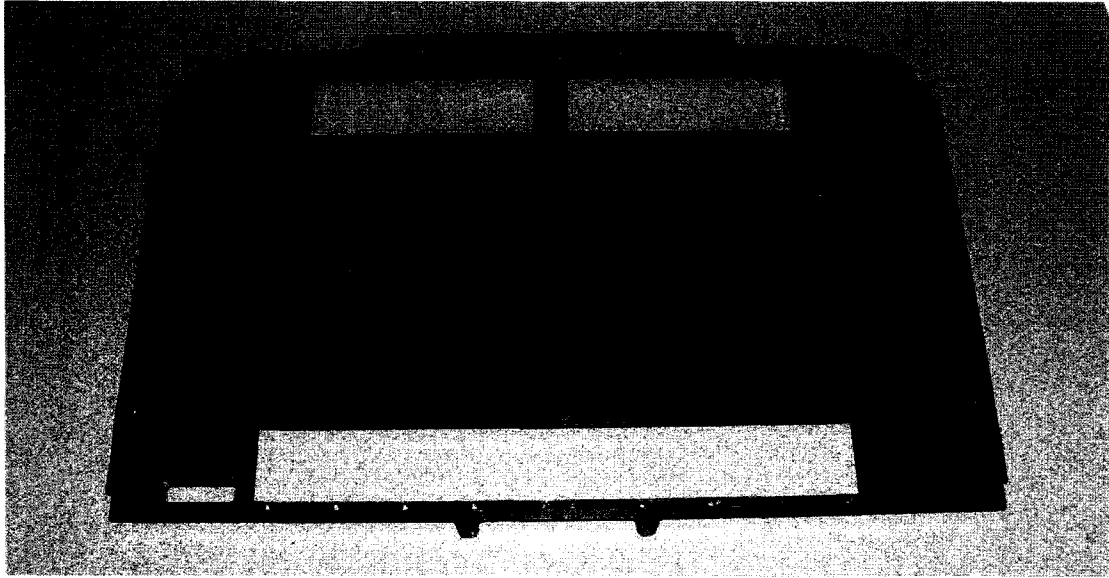


Figure 19: Aluminum Thermal Frame with Black Anodize Surface Finish

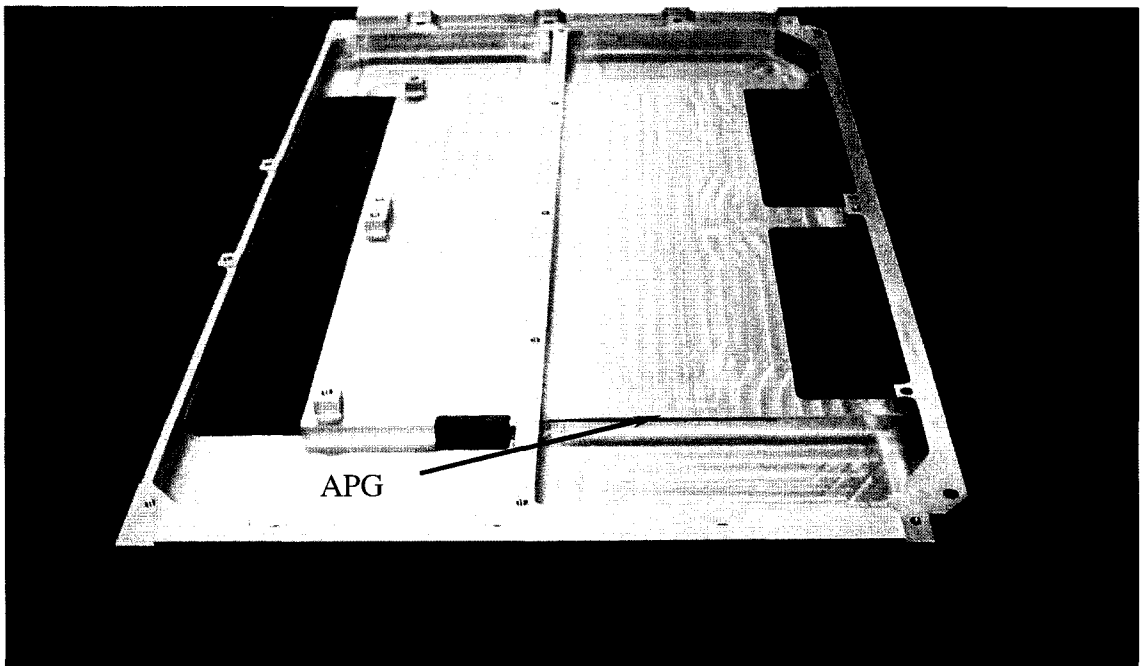


Figure 20: APG/Aluminum Composite Thermal Frame (Mid-Section APG Visible)

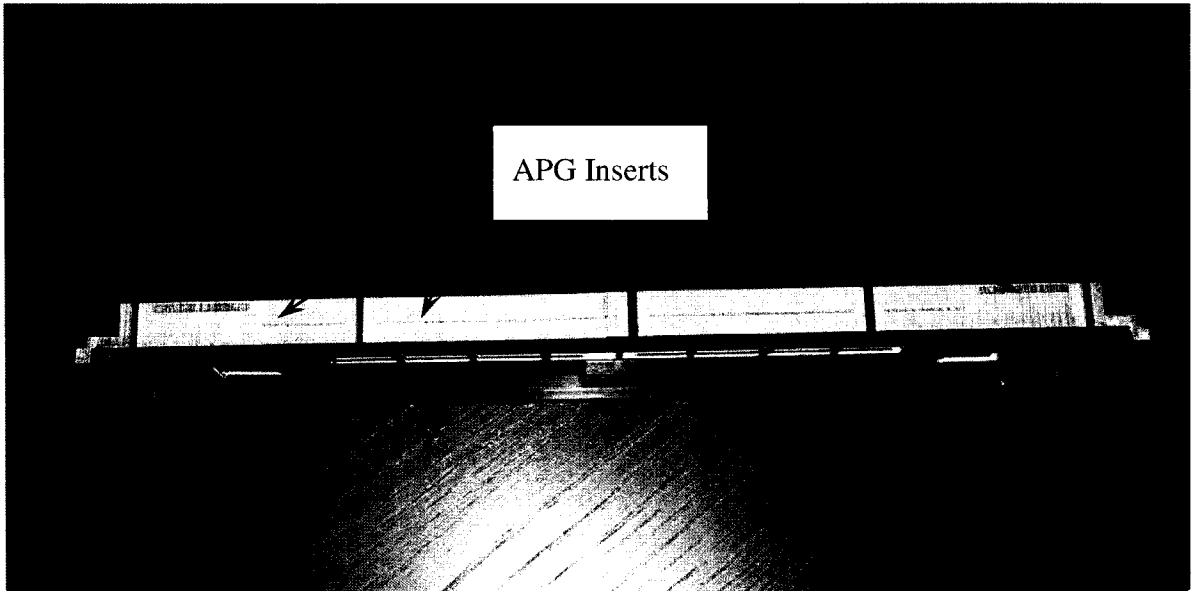


Figure 21: APG/Aluminum Composite Thermal Frame Cross-Section (APG Inserts Visible)

6.1.2 Test Setup

The test equipment consisted of resistive type Kapton heater elements with adhesive backing, K-type thermocouples and datalogger, variable voltage DC power supplies, fiberglass insulation, temperature controlled environmental chamber, and a test fixture that provided a representative conduction cooled environment for VME circuit cards.

Both test specimens were fitted with four Kapton resistive heating elements placed in locations that mimicked the placement of heat flux regions in the finite element analysis, these are shown in Figure 25 along with the placement of temperature monitoring thermocouples. The thermocouples were placed such that the approximate maximum temperature of the specimen could be obtained (near the centre), as well as at the equal spans of the specimen between the middle and edge where two thermocouples were placed. The edges of the specimen were in contact with the test fixture such that heat

flowed from the middle of the specimen to both edges and were fastened using expansion wedge locks which provide approximately 500lbs of compressive force to the interface between the test fixture and test specimens to maximize contact conductance.

The fixture has two slots so both test specimens were installed in the fixture at the same time (See Figure 22) and fiberglass insulation was placed between and around the specimens to minimize parasitic heat loss from convection, radiation and conduction into the surrounding air (See Figure 23). Covers were then installed to further reduce parasitic heat loss (See Figure 24). The primary mode of heat transfer is conduction throughout the test specimen into the test fixture where large external plate fin heat sinks were used to reject the heat to the surrounding ambient air. The fixture was placed inside an environmental chamber capable of controlling the ambient temperature over a wide range, thus allowing the specimens to be tested over a range of temperatures to explore the temperature dependence of the APG material thermal conductivity.

The four Kapton heaters bonded to each specimen were of approximately equal electrical resistance and were connected in parallel to the variable DC power supplies such that voltage could be adjusted and total power dissipation calculated using Ohm's law.

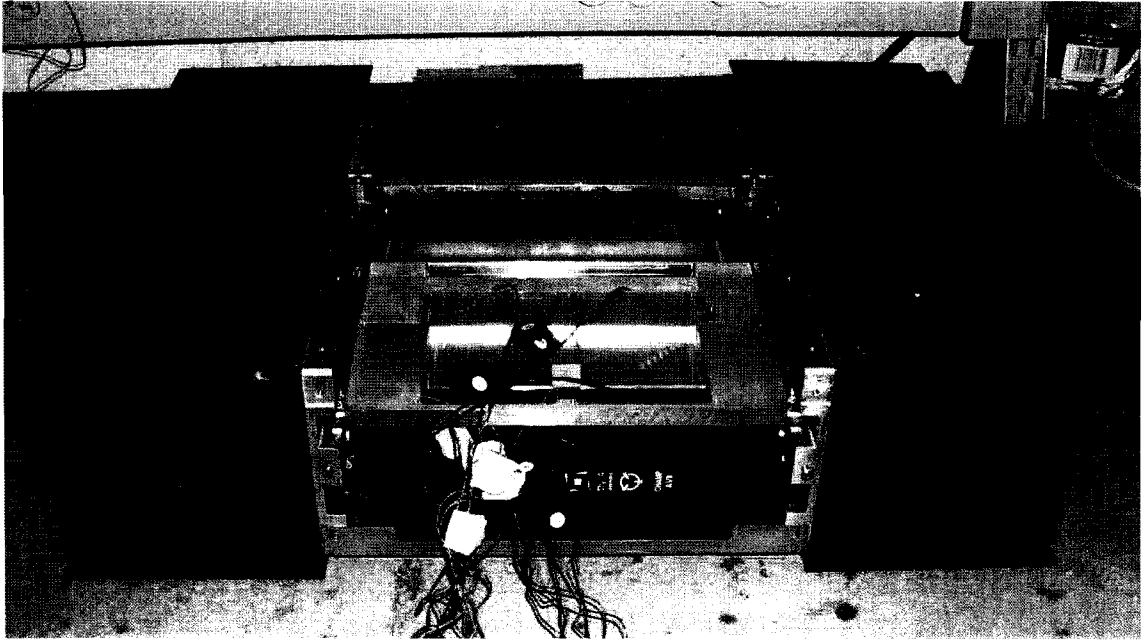


Figure 22: Test Specimens Installed in Test Fixture



Figure 23: Test Specimens Installed in Test Fixture and Surrounded with Insulation

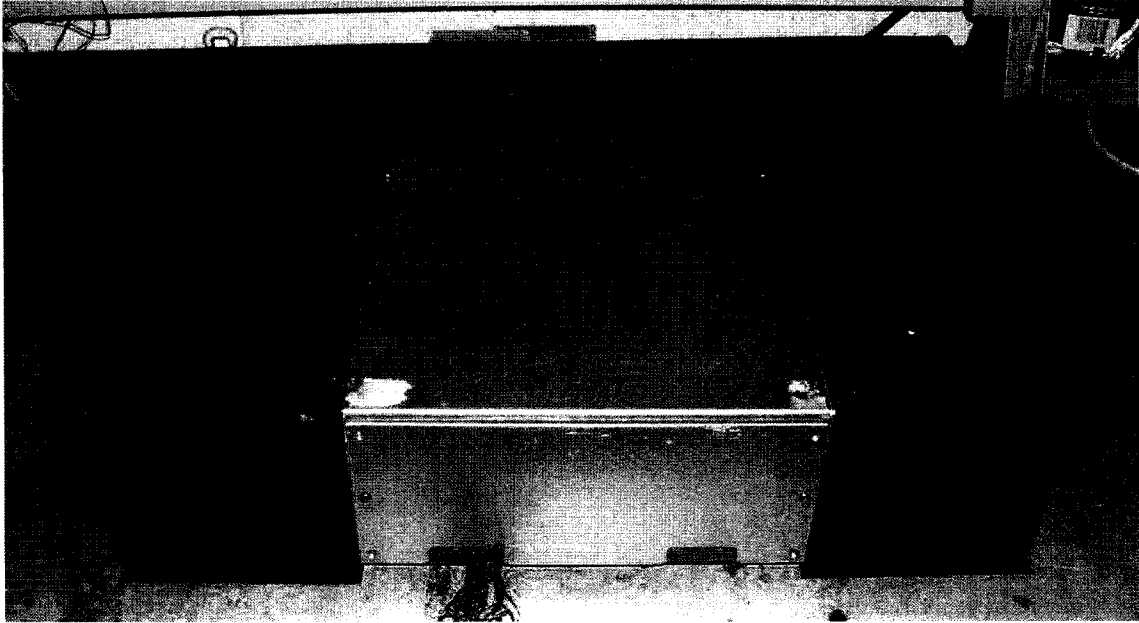


Figure 24: Test Specimens Installed in Test Fixture with Covers Installed

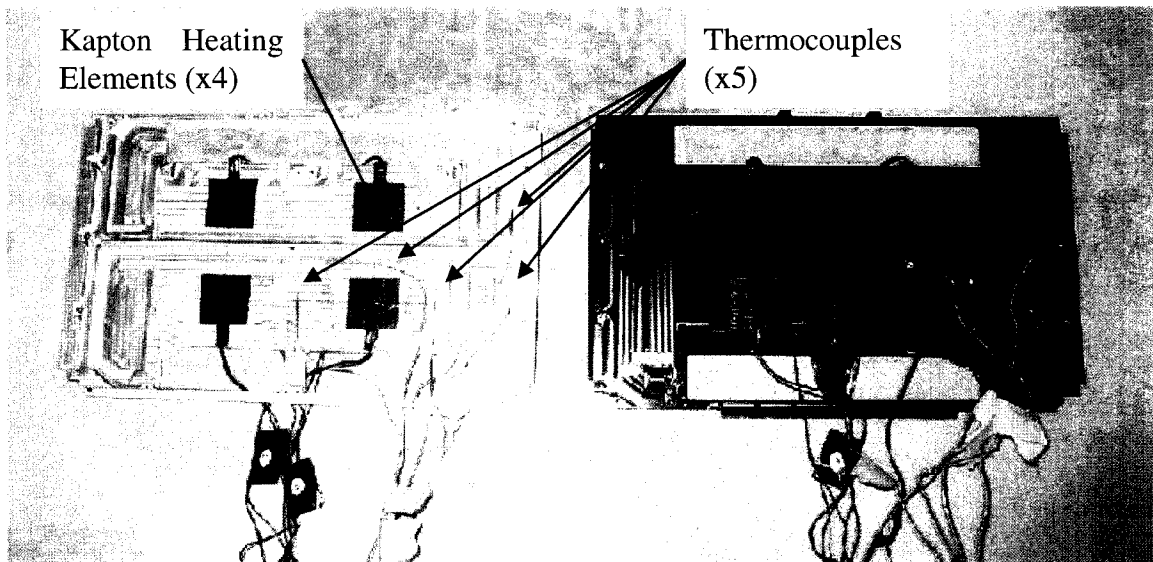


Figure 25: Composite (Raw Aluminum finish) and All-Aluminum (Black Anodized Finish) Frames with Heater Elements and Thermocouples Attached

6.1.3 Assumptions

There are several assumptions made during the thermal testing of the test specimens that could affect the accuracy of the results and comparison to Finite Element Analysis results, these are listed below:

1. **Effects of black anodize finish are neglected.** The all aluminum specimen had a black anodized surface treatment typical for manufactured aluminum piece parts to prevent corrosion and oxidation. The composite specimen had no such surface treatment. While the thermal conductivity of anodized surface treatments is reported to be very low, $0.5 - 1.0 \text{ W/m K}^{15}$, the typical thickness is on the order of only 0.1 - 1 mils ($\sim 0.0025 - 0.025 \text{ mm}$). For the purpose of testing the surface treatment effects were ignored. The actual thermal performance of the all aluminum specimen would therefore be higher if no treatment was used and as such the relative comparison with the composite specimen would be marginally less.
2. **Heat flux of heating elements equals I^2R .** The heat flux of the Kapton heating elements is assumed to be equal to the product of the parallel resistance of the heating elements and the square of the current supplied by the DC power supplies. This ignores any inaccuracy in the power supply reading and losses in the lead wires.
3. **Parasitic is minimized through use of insulation.** The test specimens were wrapped with fiberglass insulation during testing to minimize heat loss through

radiation, convection and conduction into the surrounding air. Parasitic heat loss is not eliminated but the test results can be correlated to Finite Element Analysis for the known aluminum material and the test results adjusted to account for this source of error.

4. **Thermocouples are accurate and in intimate contact.** The Type K thermocouples used for temperature measurements are assumed to be accurate and in intimate contact with the test specimen at all times. Kapton tape was used to secure the thermocouples and each was checked between tests to ensure contact was maintained.
5. **Aluminum 6061T6 thermal conductivity equals that of the thermal analysis.** For comparative purposes the thermal conductivity of aluminum 6061T6 is assumed to be 167 W/m K for the Finite Element Analysis and the actual test specimens.
6. **Thermal Steady State is achieved.** For the purpose of testing, thermal steady state is considered to be achieved when the average temperature change of the test specimen is less than 0.2 °C in 10 minutes.

6.1.4 Test Sequence

The first set of tests were performed at room ambient temperature conditions using a range of total power dissipation, 20, 40, and 60 W, total for each of the two specimens. Power was applied at 20 W and the temperatures recorded once per minute until steady-state was reached. Power was then increased to 40 W and 60 W respectively, allowing

sufficient time for steady state to be achieved at each level. This sequence was repeated separately for both the aluminum and APG test specimens.

A second set of tests were performed in a similar manner as described above but the entire test sequence was performed over a range of ambient temperatures from -50 to 100°C inside an environmental temperature chamber. The range was chosen to be representative of temperatures experienced in typical military electronics applications. While the ambient temperature was controlled the average temperature of each test specimen varied with power dissipation and material, i.e. the average temperature of the aluminum test specimen at 60 W and -50°C ambient was higher than the average temperature of the APG specimen for the same given test conditions.

6.1.5 Results

6.1.5.1 Constant Ambient Temperature

The results of the ambient room temperature testing are illustrated in Figure 26. Temperature measurements were taken at various points on the test specimen including two at the edge where the specimen was clamped to the fixture. These two edge measurements were used as the reference to the other measurements. The graph illustrates the temperature rise from the average of the two edge measurements to the centre measurement on the specimen assumed to be the maximum temperature.

Both the aluminum and APG results are shown for comparison purposes. The data illustrates a linear relationship between power dissipation and temperature rise as

expected. A linear regression line is fitted to each dataset and the equations of the linear fit lines are shown on the graph. The difference between the slopes of these lines represents the improvement in performance for the APG specimen over the aluminum specimen. The percentage improvement can be calculated as:

$$\%_{\text{improvement}} = \frac{\text{Slope}_{Al} - \text{Slope}_{APG}}{\text{Slope}_{Al}} \times 100\% = \frac{0.6565 - 0.4186}{0.6565} \times 100 = 36\%$$

Equation 3: Percentage Thermal Improvement of APG over Aluminum

This is less than expected based on the results of the finite element analysis presented in Section 4.2.6 where results indicated that the APG specimen would result in an improvement of approximately 57%.

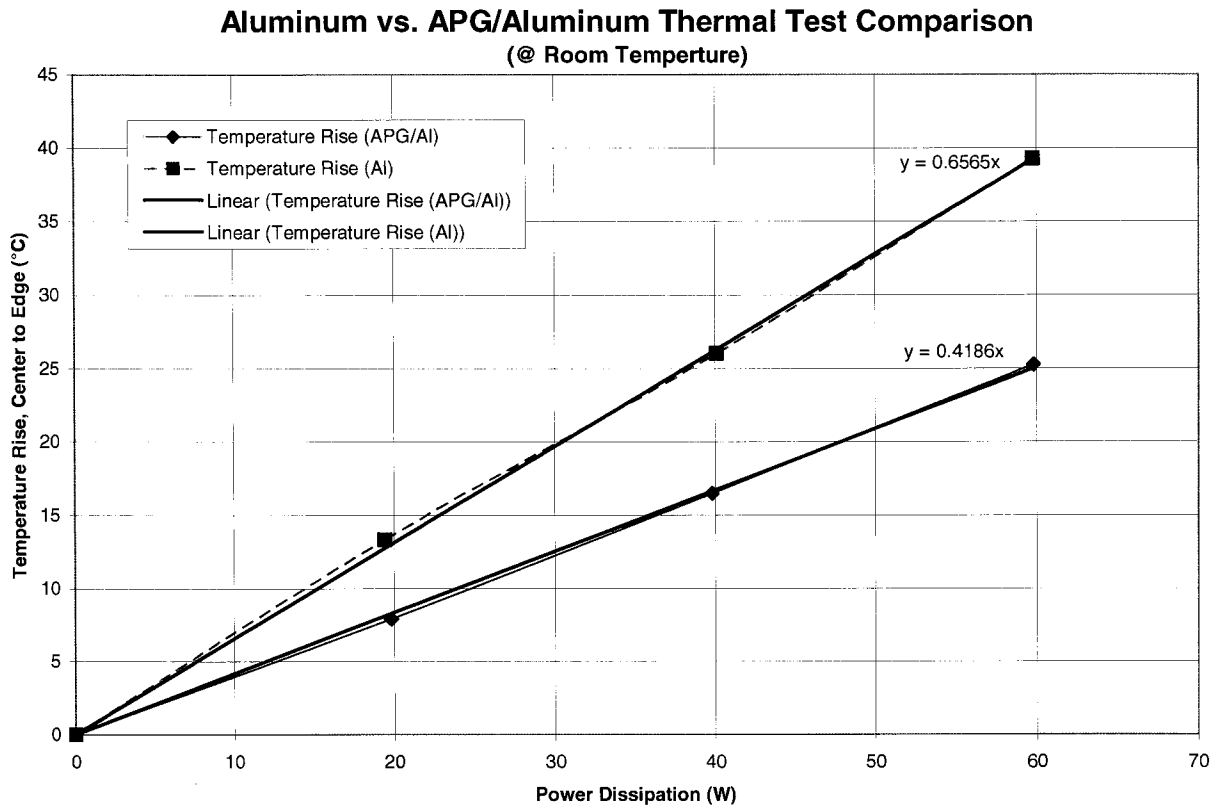


Figure 26: Thermal Test Results for Al and APG/Al Test Specimens at Room Ambient Temperature with Varying Power Dissipation

6.1.5.2 Varying Ambient Temperature

The results of the testing performed over a range of ambient temperatures are presented in Figure 27 for the aluminum specimen and Figure 28 for the APG specimen. The data has been presented in such a way to show the relationship between ambient temperature and temperature rise in the specimen for each of the three power dissipations tested and include linear regression lines. The thermal conductivity of Aluminum is generally not temperature dependant in the test range; however, the non-zero slopes of the regression lines in Figure 27 indicate a temperature dependence in the data which may be related to

the test set up or methodology. It should be noted that each of the three sets of data exhibit similar slopes which decrease with increasing power dissipation and have an average of -0.0205.

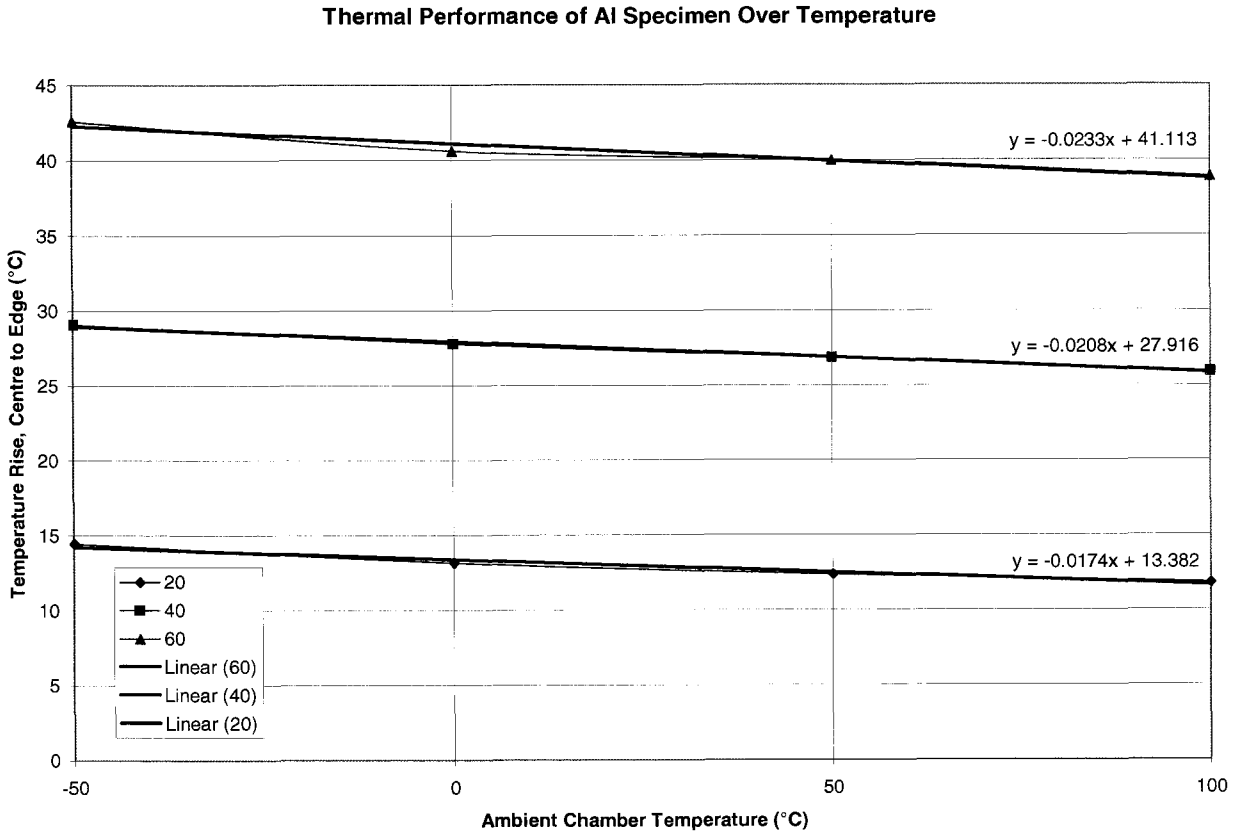


Figure 27: Aluminum Test Specimen Results with Varying Ambient Temperature

The thermal conductivity of APG is reported to be temperature dependant in the literature. The slopes of the regression lines shown in Figure 28 increase with increasing power and have an average of 0.0195. The positive slope of the APG dataset compared to the negative slope of the aluminum dataset indicates a strong temperature dependence of the thermal conductivity of the APG material.

Thermal Performance of APG/Al Specimen Over Temperature

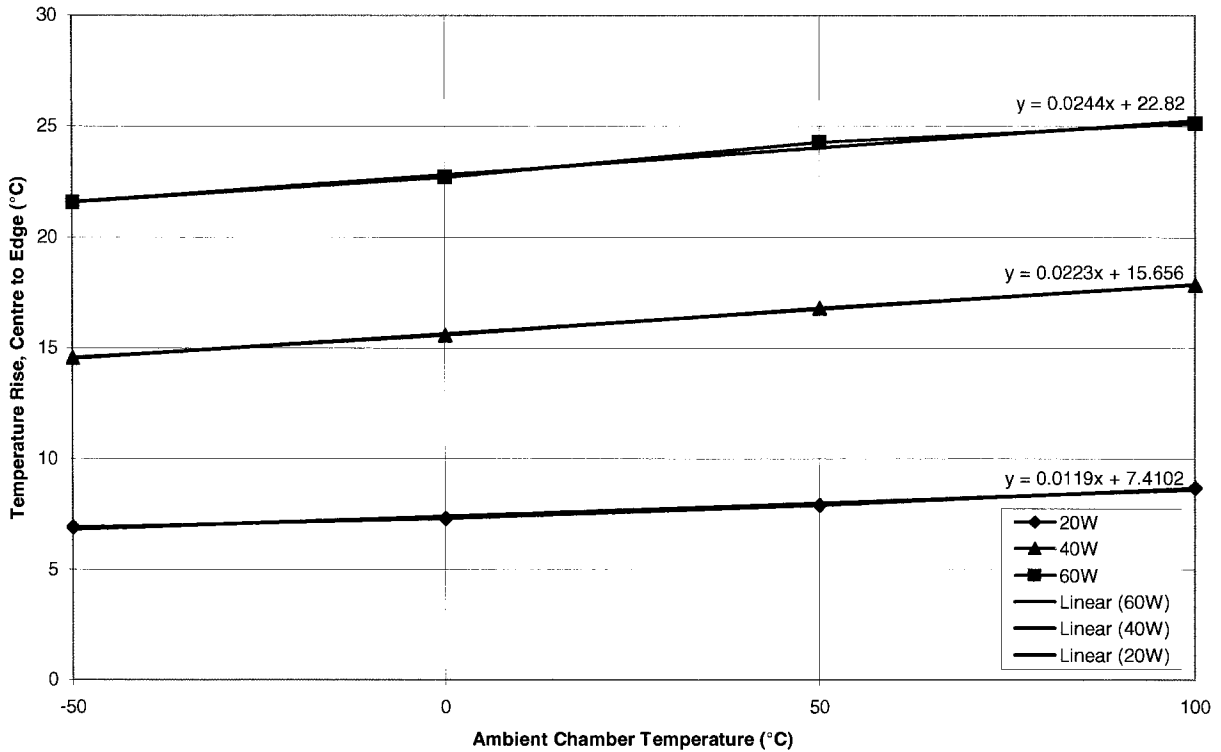


Figure 28: APG/Al Test Specimen Results with Varying Ambient Temperature

6.1.6 Discussion

The test results presented in Section 6.1.5.1 indicate a disagreement with the Finite Element Analysis results presented in Section 4.2.6 for both the aluminum and APG specimens. Figure 29 illustrates the comparison between test and FEA data.

Aluminum vs. APG/Aluminum Thermal Test Comparison with FEA Results Included (@ Room Temperature)

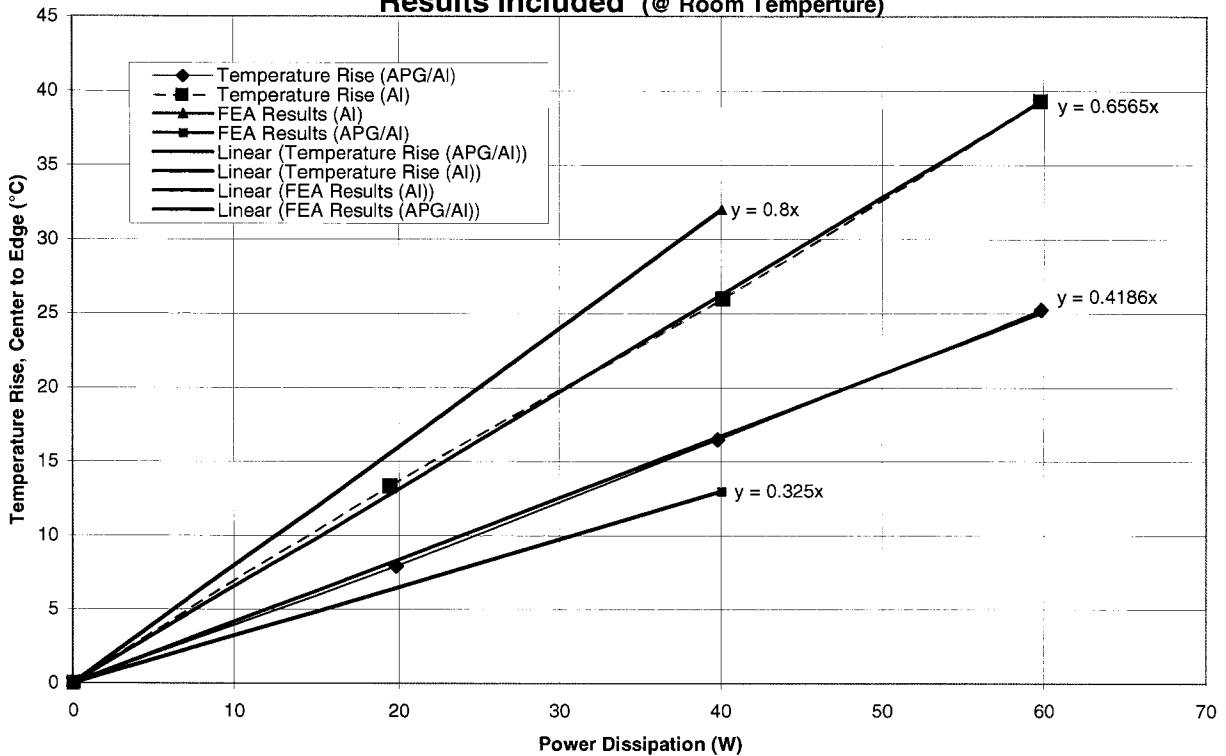


Figure 29: Comparison of FEA and Test Results

Examining the results for the aluminum cases it is observed that the test data indicates a lower temperature rise when compared to the FEA results for equivalent power dissipation. Assuming that all conditions are equal, i.e. geometry, thermal conductivity, heat flux, and temperature measurement points, this discrepancy represents the parasitic heat loss from the test set up. Therefore a correction factor can be calculated to account for the parasitic heat loss of the test setup. Numerically this is represented by the difference between the slopes of the test and analysis results lines and is calculated as:

$$Parasitic_Loss_Correction = Al_Slope_{FEA} - Al_Slope_{Test} = 0.8x - 0.6565x = 0.1435x$$

Equation 4: Parasitic Heat Loss Correction Factor

Examining the results for the APG cases it is noted that an opposite trend exists between the FEA and test results, i.e. the test data indicates a higher temperature rise than the FEA data. Assuming all other factors being equal, including the parasitic heat loss in the test set up, this discrepancy is attributable to the thermal conductivity of the APG material. The data indicates that the thermal conductivity of the APG is less than 1530 W/m K as reported by the manufacturer.

In order to estimate the actual thermal conductivity of the APG material, the test data and parasitic heat loss correction factor can be used to determine the anticipated FEA results per Figure 29. Assuming that the parasitic heat loss is equivalent for each test specimen for a given average temperature of that specimen, the first step is to select a temperature at which to determine the difference between the test and FEA results. For convenience, 25°C is selected as it correlates to 60 W on the APG test curve. The second step is to determine the temperature difference between the aluminum test and FEA results at 25°C, this is accomplished using Equation 4 and results in a temperature difference of 5.5°C. Next, this temperature difference is added to the APG test results at 25°C for a total of 30.5°C. A new line can now be drawn through the origin and “30.5°C, 60 W” which represents the anticipated temperature rise for the APG FEA model as shown in Figure 30.

Aluminum vs. APG/Aluminum Thermal Test Comparison with Corrected APG FEA Results

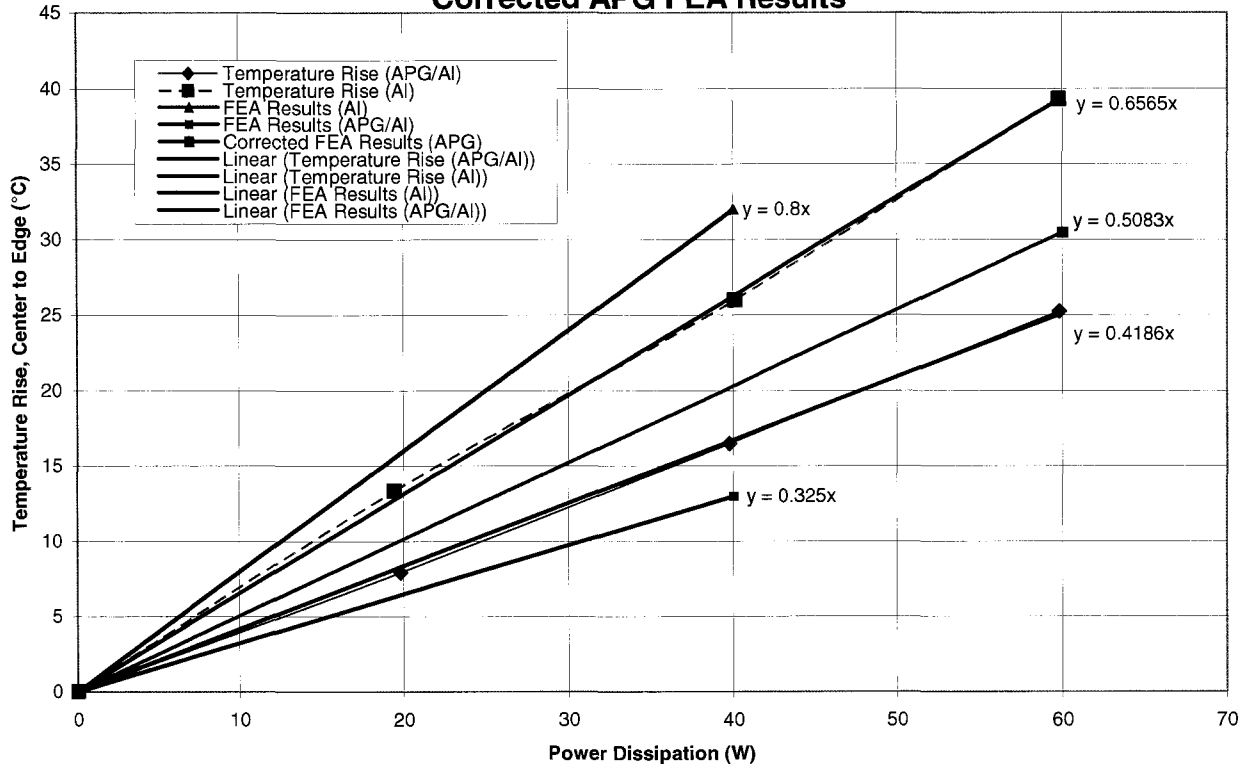


Figure 30: Corrected APG FEA Results

Finally, using the equation of the corrected FEA results shown, $y = 0.5083x$, for $x = 40$ W, the temperature rise equals 20.3 °C.

Returning to the Finite Element Model, the following curve, Figure 31, was developed for the APG model with varying APG in-plane thermal conductivity and constant orthogonal thermal conductivity at 40 W power dissipation.

Effect of APG Thermal Conductivity on FEA Model Temperature Rise (@ 40 W)

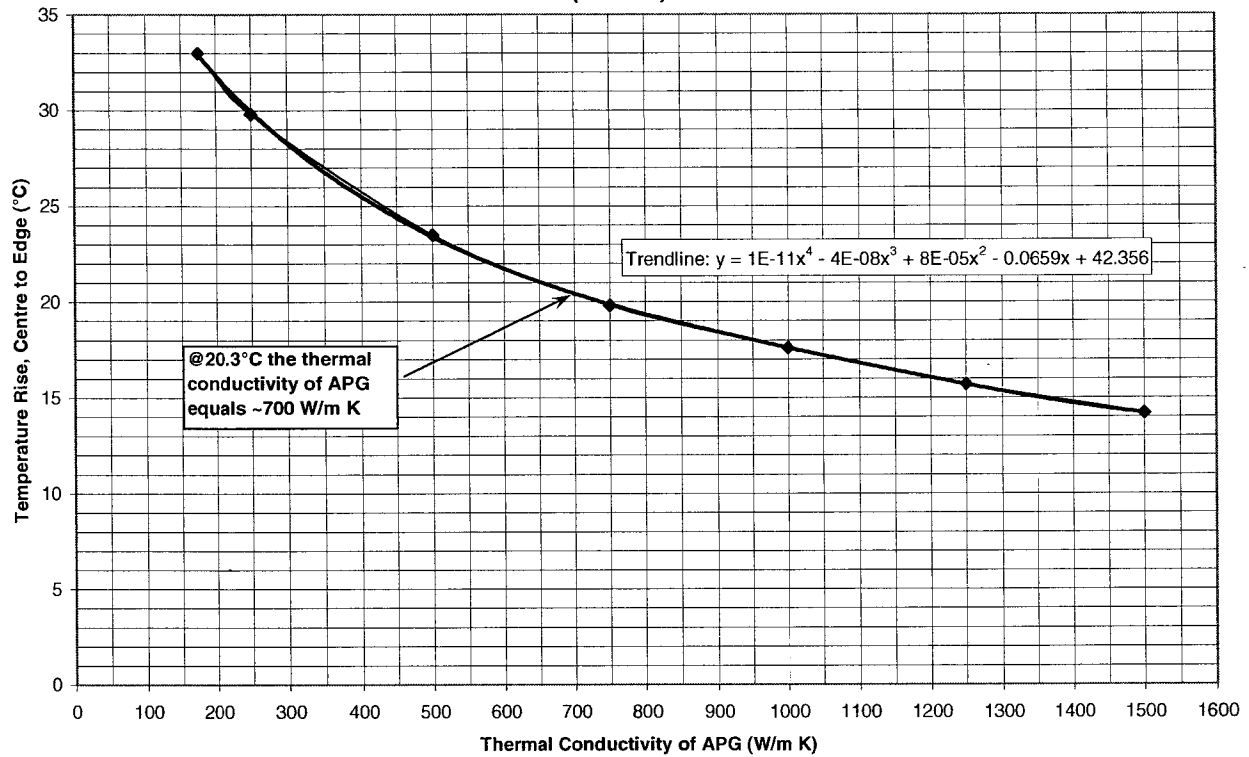


Figure 31: Effect of In-Plane Thermal Conductivity on APG Thermal Results at 40 W

Using the corrected temperature rise of 20.3°C and the curve above, the thermal conductivity of the APG material can be estimated as 700 W/m K. The curve presented in Figure 31 illustrates two interesting observations, firstly, the knee of the curve lies in the range of approximately 600 – 700 W/m K and therefore the biggest improvement in thermal performance is gained with a thermal conductivity equal to or greater than this range of values, secondly, the curve is relatively shallow in the vicinity of 700 W/m K and therefore very sensitive to the temperature value selected. Assuming a relatively small error of +/- 1°C in the temperature value of 20.3°C results in an error of approximately +/- 100 W/m K in the thermal conductivity of the APG material, putting it in the range of 600 - 800 W/m K at ambient room temperature conditions.

The results of the temperature testing with varying ambient temperature from -50 to 100°C indicated strong temperature dependence. This indicates that the thermal conductivity varies with temperature. The test results for the room temperature, -50°C and 100°C cases are shown in Figure 32 below. Using the methodology discussed in the previous paragraphs the thermal conductivity can be estimated for the extreme cases of -50°C and 100°C. These values turn out to be approximately 950 W/m K and 640 W/m K respectively. Unfortunately, the higher thermal conductivity occurs at lower temperatures where it is not required for electronics cooling applications.

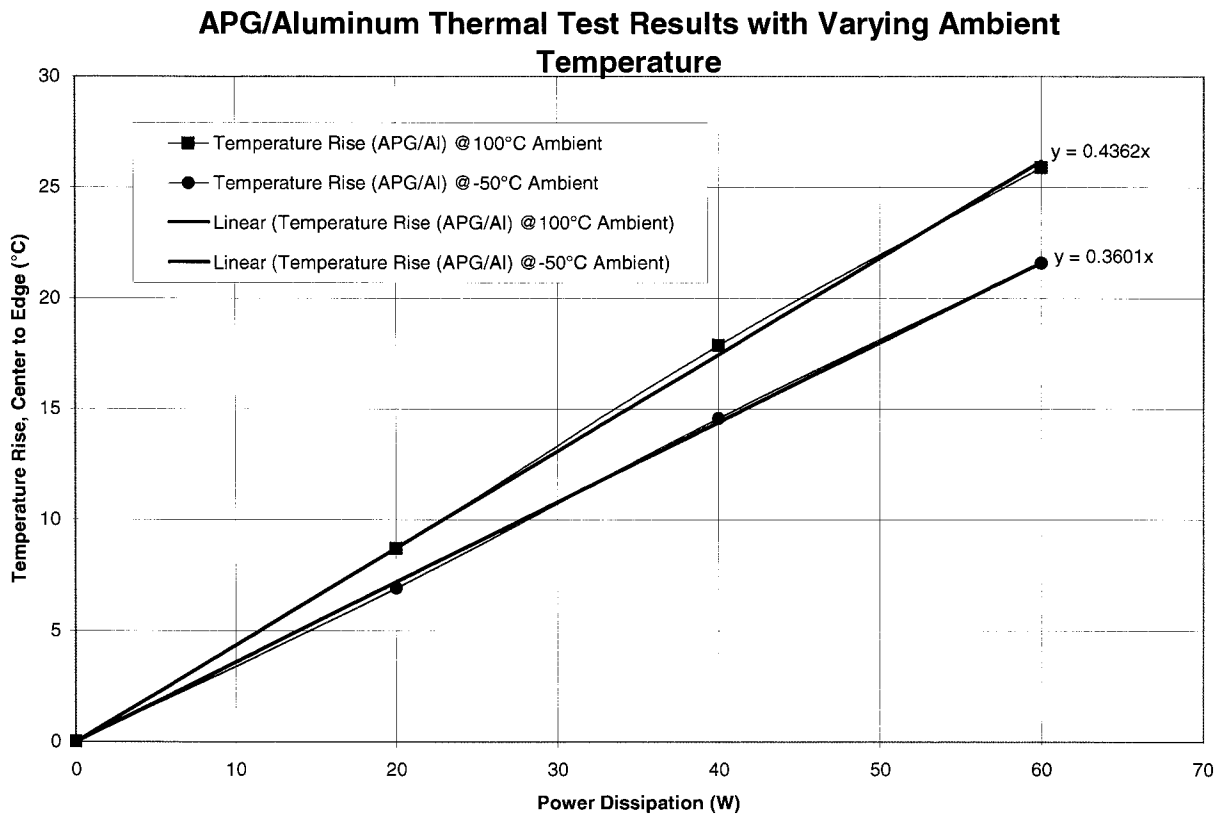


Figure 32: APG Thermal Test Results with Varying Ambient Temperature

6.2 Sectioned Sample Testing

In an effort to verify the thermal conductivity of the APG material a second method to measure the thermal conductivity was devised. This involved cutting sections out of the second APG/Al composite prototype frame and stacking them side by side such that the APG and aluminum sections were parallel to one another. The multi-layer sandwich of sections was then subjected to a heat flux and the temperature drop across the sandwich measured in order to back calculate the thermal conductivity of the APG given the known conductivity of the aluminum. This testing was performed at the University of Waterloo's Microelectronics Heat Transfer Lab (MHTL).

6.2.1 Test Specimen

The test specimens are shown in the following pictures. Figure 33 shows the Prototype frame with sections removed. Figure 34 shows the un-laminated test sections. Figure 35 shows the laminated test sections. Two thickness of APG material can be observed, these are taken from two different areas of the frame.

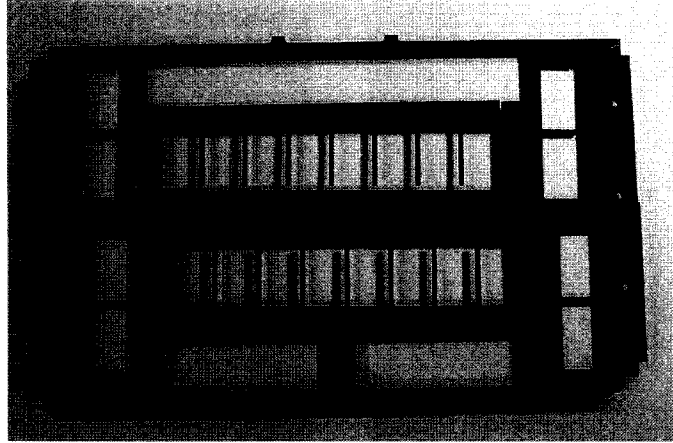


Figure 33: APG Composite Prototype 2 with Sections Removed

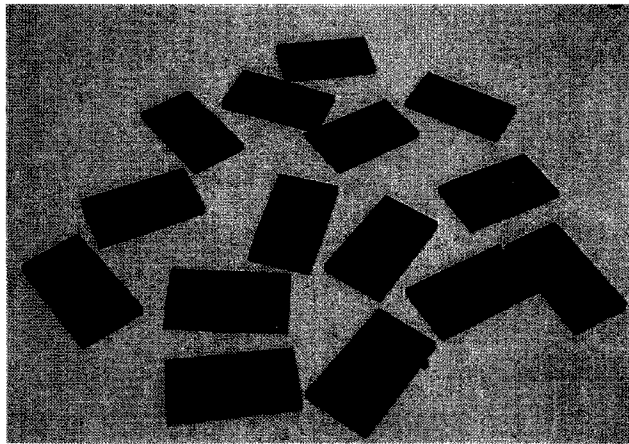


Figure 34: APG Sections Removed From Prototype

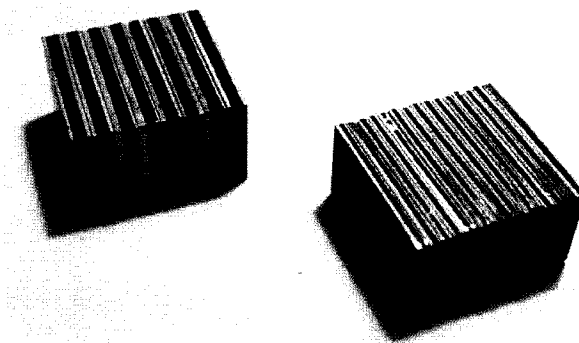


Figure 35: APG Section Laminated Together, Two Thicknesses of APG

6.2.2 Test Setup and Procedure

For a complete summary of the set up, procedure and results refer to the paper included in APPENDIX A .

6.2.3 Discussion

The results of the testing concluded that the effective thermal conductivity of the APG material is in the range of approximately 200 – 300 W/m K. Those results are in sharp disagreement with the results presented in this study and may suggest that delamination of the sections during cutting may have resulted in large thermal interface resistances affecting the results. Also, due to the small temperature gradients and potential error in test and measurement it is unlikely that these results are accurate.

6.3 Industry Experience

While published industry data and experience is scarce, one paper published by Shuhua Zhang of the American Competitiveness Institute discusses similar testing to that presented in this study¹⁶. In his paper, Zhang performs thermal testing of APG/aluminum composite plate and compares the results with an equivalent aluminum plate. The methodology was similar to that employed in this study but the test specimen was heated at one end with a resistive element and cooled at the other by clamping to a single large heat sink. Insulation was used to minimize parasitic heat loss and thermocouples were used to measure temperature rise across the specimen.

The Al/APG specimen is a simple plate measuring 5.5” x 5.5” x 0.120” and made up of 0.080” APG sandwiched between 0.020” thick layers of aluminum. Zhang concluded that the effective thermal conductivity of the combined Aluminum/APG composite was 540 W/m K. However, there was no attempt to correct for the parasitic heat loss. This value is again in contrast with manufacturer data. In order to estimate the thermal conductivity of the APG material itself in Zhang’s experiment it is necessary to factor out the effect of the aluminum which Zhang assumes to have a thermal conductivity of 200 W/m K. This can be accomplished by calculating the thickness fraction of the aluminum and APG and solving for the thermal conductivity of the APG using the following equation:

$$K_{Effective} = \frac{T_{Al}}{T_{Total}} \times K_{Al} + \frac{T_{APG}}{T_{Total}} \times K_{APG}$$

Equation 5: Effective Thermal Conductivity of APG/AL Composite Plate

Substituting known values for thermal conductivities and thicknesses and solving for the thermal conductivity of the APG yields a value of 710 W/m K. This value is extremely close to the value determined by this study and is well within the range of error. Therefore, the work performed by Zhang substantiates the work presented herein.

6.4 Conclusions

Thermal testing has indicated that the thermal conductivity of the APG material is approximately 700 W/m K at room temperature. Testing has confirmed that the thermal conductivity of the APG decreases with increasing temperature and varies between

approximately 640 W/m K and 950 W/m K over the useful temperature range for electronics cooling applications. These results indicate that the thermal conductivity is much lower than reported by the manufacturer (minimum 1530 W/m K) by more than half. However, the thermal performance of a composite APG/aluminum structure is not linearly dependant upon the thermal conductivity of the APG alone and when it is combined as a composite with aluminum much of the benefit of the APG can be had for much lower thermal conductivity than reported by the manufacturer.

7 Other Environmental/ Mechanical Considerations

In addition to high thermal conductivity, technologies utilized in the conduction-cooling of rugged electronics assemblies must be able to withstand other environmental factors such as shock and vibration, humidity, corrosive environments, thermal cycling, fungal growth, etc. Also, consideration must be given to mechanical properties such as weight, Coefficient of Thermal Expansion (CTE), stiffness and warpage.

7.1 Environmental Considerations

One of the most important environmental conditions that affect rugged electronics is high level shock and vibration. Shock levels of 40 g, sine vibration of 10 g, and random vibration of 0.1 g^2/Hz (in the range of 15-2000 Hz) is common. Any technologies considered for rugged electronics cooling applications must be able to withstand these requirements. Both the all aluminum and the APG/aluminum composite frames were subjected to a 2 g Sine sweep and 0.1 g^2/Hz random vibration input to compare their frequency response over the range of 15 – 2000 Hz in comparison to the all aluminum design. Figure 36 through Figure 41 illustrate those response curves.

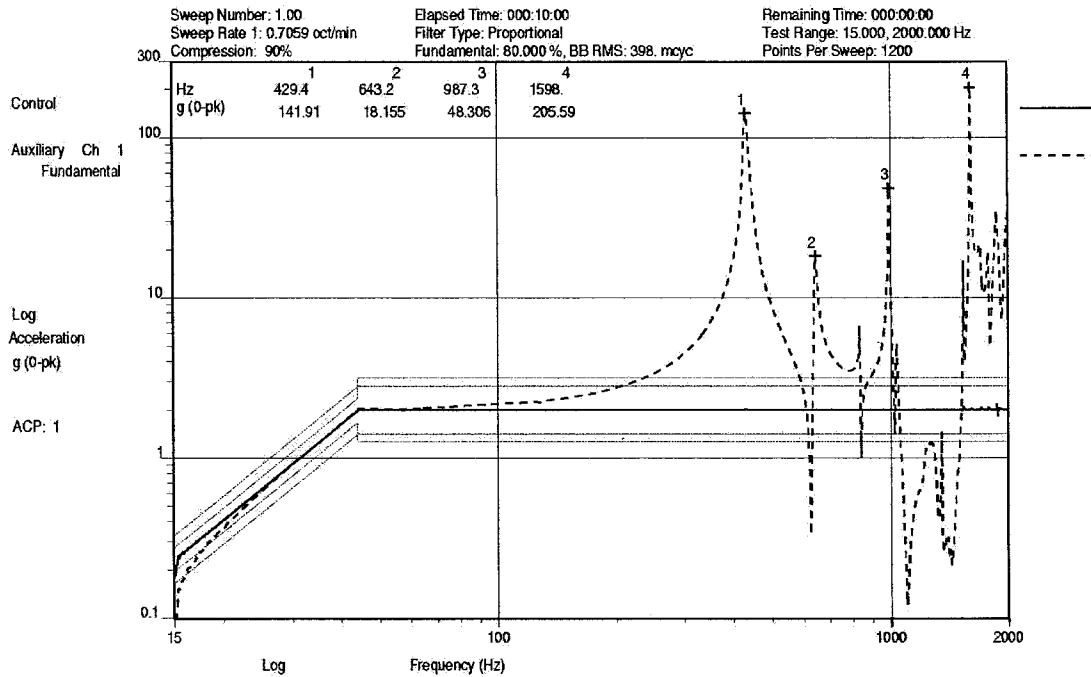


Figure 36: Sine Sweep Response, All Aluminum Frame (2 g input, 15-2000 Hz)

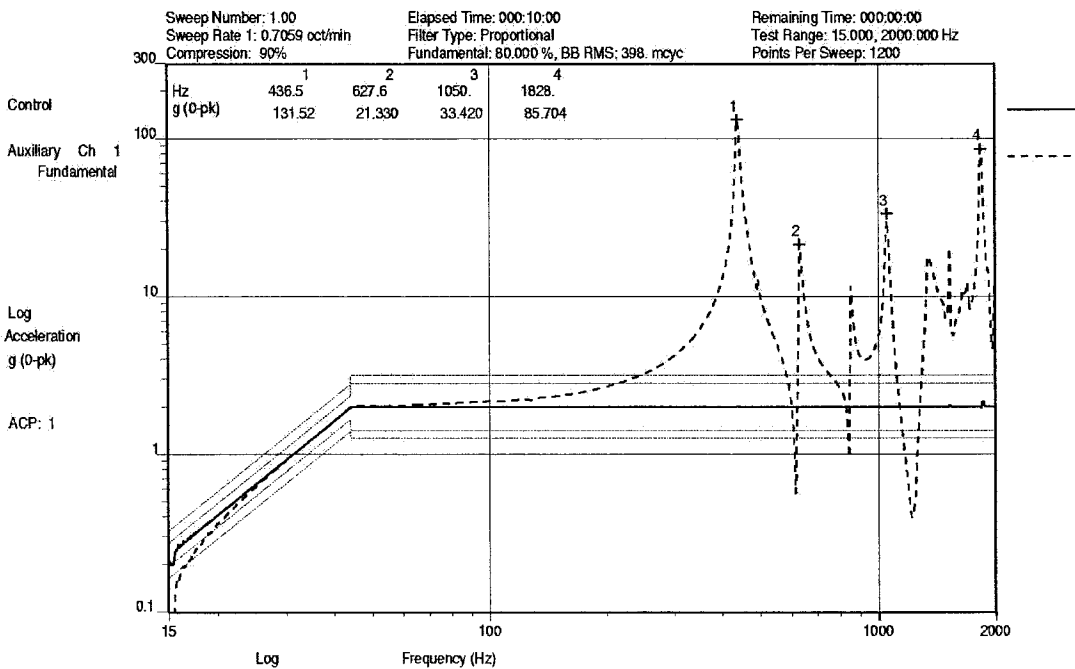


Figure 37: Sine Sweep Response, APG/Aluminum Frame #1 (2 g input, 15-2000 Hz)

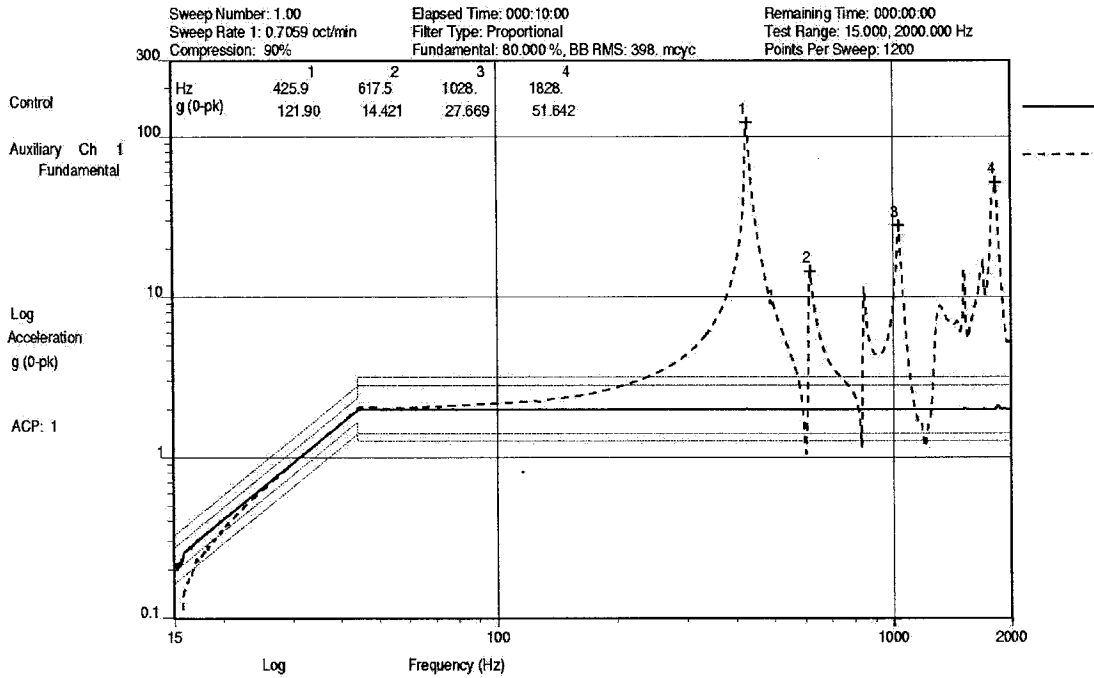


Figure 38: Sine Sweep Response, APG/Aluminum Frame #2 (2 g input, 15-2000 Hz)

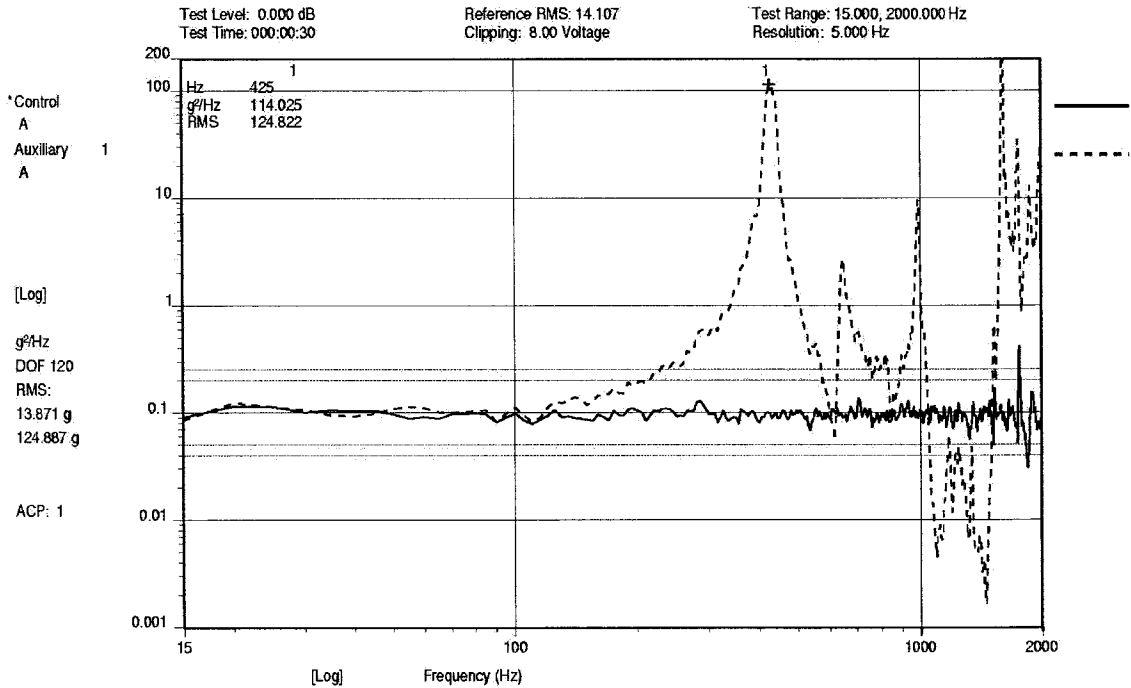


Figure 39: Random Vibration Response, All Aluminum Frame (0.1 g²/Hz, 15-2000 Hz)

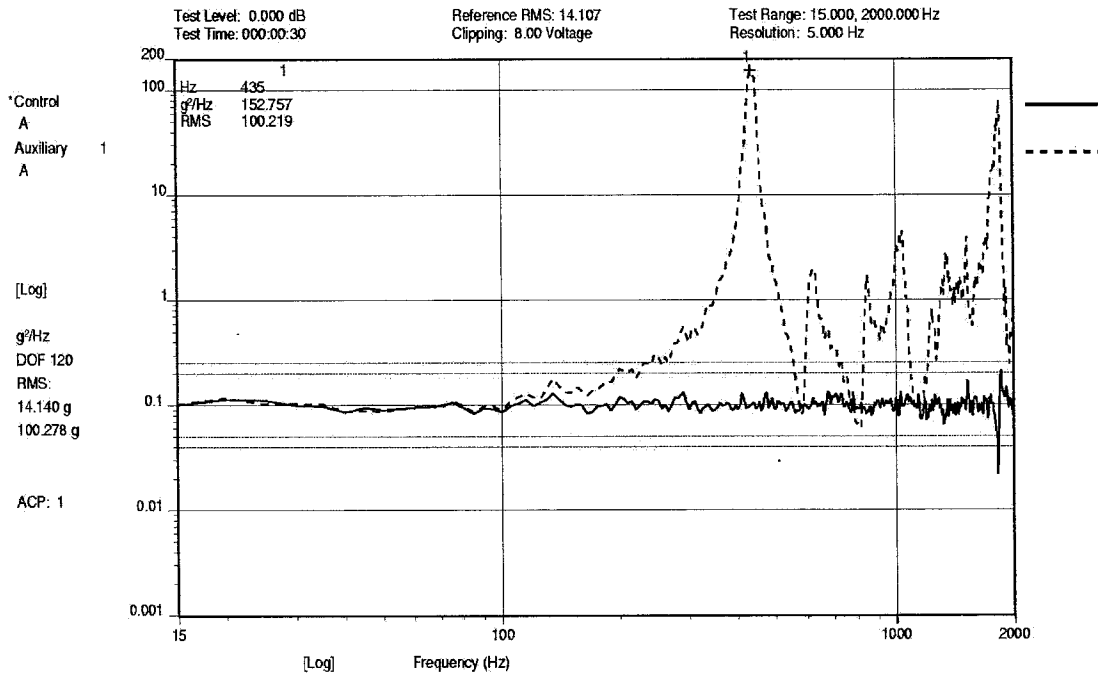


Figure 40: Random Vibration Response, APG/Aluminum Frame #1 (0.1 g^2/Hz , 15-2000 Hz)

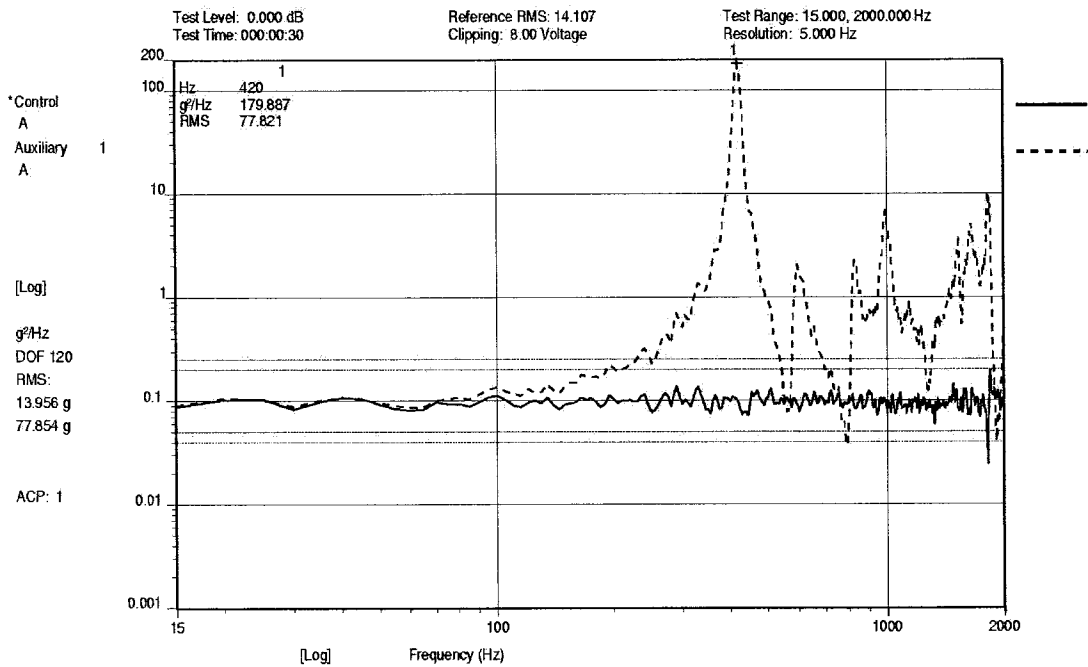


Figure 41: Random Vibration Response, APG/Aluminum Frame #2 (0.1 g^2/Hz , 15-2000 Hz)

Examining the response of the Sine sweep in Figure 36 the first mode response of the all aluminum frame occurs at 429 Hz with a magnitude of 142 g, subsequent significant modes occur at 643 Hz, 987 Hz, and 1598 Hz with magnitudes of 18 g, 48 g, and 206 g. Examining the response of the Sine sweep in Figure 37 the first mode response of the first APG/aluminum frame occurs at 437 Hz with a magnitude of 132 g, subsequent significant modes occur at 628 Hz, 1050 Hz, and 1828 Hz with magnitudes of 21 g, 33 g, and 85 g. Examining the response of the Sine sweep in Figure 38 the first mode response of the second APG/aluminum frame occurs at 426 Hz with a magnitude of 121 g, subsequent significant modes occur at 618 Hz, 1028 Hz, and 1828 Hz with magnitudes of 14 g, 28 g, and 52 g. Comparing these responses, it can be noted that the first mode response of the APG/aluminum frames falls both above and below that of the all aluminum frame. Subsequent modes are similar with the exception of the fourth significant mode which is significantly higher in frequency for the APG/aluminum frames and has an average magnitude of 69 g compared to 206 g for the all aluminum frame. In general, higher frequencies and lower responses are desired.

Examining the random vibration responses of the all aluminum frame in Figure 39 the magnitude of the response is $114 \text{ g}^2/\text{Hz}$ at 425 Hz and the total RMS (Root Mean Square) response, over the entire frequency band, is $125 \text{ g}_{\text{rms}}$. Examining the random vibration responses of the first APG/aluminum frame in Figure 40 the magnitude of the response is $153 \text{ g}^2/\text{Hz}$ at 435 Hz and the total RMS response, over the entire frequency band, is $100 \text{ g}_{\text{rms}}$. Examining the random vibration responses of the second APG/aluminum frame in Figure 41 the magnitude of the response is $180 \text{ g}^2/\text{Hz}$ at 420 Hz and the total RMS response, over the entire frequency band, is $78 \text{ g}_{\text{rms}}$. Again, the responses of both frame

type are similar at the first mode in terms of frequency but in this case the APG/aluminum frames exhibit higher response at this point. The APG/aluminum frames exhibit lower total response over the entire frequency range compared to the all aluminum frame which is generally more desirable. Overall, there is little difference between the vibration responses of the all aluminum and APG/aluminum frames.

Another consideration for rugged electronics is thermal cycling. Typical rugged environments expose the electronics to multiple thermal cycles for a variety of conditions including during manufacturing, repair, operation and storage. The prototype APG/aluminum frame was subjected to 500 cycles from -40 to 125°C with no obvious mechanical degradation.

Other environmental factors such as humidity, corrosive environments (salt fog, fluids contamination), and fungal growth may be present in rugged electronics applications. Since the composite design requires that the APG material be completely encapsulated within the parent material, these environmental conditions are handled by the parent material itself and the use of effective surface treatments such as plating or anodizing.

7.2 Mechanical Property Considerations

Many rugged electronics applications, particularly Avionics, are sensitive to weight. The APG has a density of approximately 2.26 g/cm³ compared to 2.7 g/cm³ for aluminum (6000 series), therefore the composite APG/aluminum will have less mass than an equivalent all aluminum design.

The CTE of APG is approximately $-1 \text{ ppm}/^\circ\text{C}$ in the in-plane directions and $25 \text{ ppm}/^\circ\text{C}$ in the through-plane directions compared to $23.6 \text{ ppm}/^\circ\text{C}$ for aluminum (6000 series). The CTE of the composite piece part is generally dominated by the parent material as the APG is decoupled at the interface between the APG and aluminum.

Properties such as stiffness and warpage are important for precise design of electronics cooling assemblies and are generally dominated by the parent material, warpage can be controlled during the manufacturing process.

8 Conclusions and Recommendations

8.1 Conclusions

This study examined the thermal conductivity of Annealed Pyrolytic Graphite and its potential application in conduction-cooled electronics applications. Finite Element Analysis was performed to examine design trade-offs and material property variations under the inherent assumption that the APG material itself had a minimum thermal conductivity of 1530 W/m K as reported by the manufacturer. Given that assumption the improvement in thermal performance was significant for a typical conduction-cooled VME circuit card thermal frame design. The proposed composite frame design offered an improvement in thermal performance of approximately 2.5X over an equivalent all aluminum frame.

Thermal testing of the prototype thermal frames was performed to benchmark the results of the FEA; however, the test results indicated that the thermal performance of the APG/aluminum composite frame was not as good as expected. Careful examination of the test data and correlation to the thermal analysis, corrected for parasitic heat loss in the test setup, indicated that the actual effective thermal conductivity of the APG material

itself lies in the range of 640 to 950 W/m K over the useful temperature range of -50 to 100°C. Published test data supports this conclusion. While this range of values is much lower than anticipated, it has been shown that a large benefit can still be realized from the use of a well designed metal/APG composite cooling structure. For the design examined in this study, an improvement of approximately 1.6X was gained.

8.2 Recommendations

It is recommended that any design requiring enhanced thermal performance beyond the capability of typical aluminum or copper metals consider the use of APG/metal composites.

Due to the large discrepancy between the measured and reported values of thermal conductivity it is recommended that a conservative value of in-plane thermal conductivity of 640 W/m K and thru-plane value of 15 W/m K, be used when performing FEA or other such thermal simulations.

Due to potentially large variations in the thermal conductivity of the APG material, prototype testing should be performed on any new design utilizing APG/metal composite designs with periodic quality control re-tests performed on a sample basis.

**APPENDIX A University of Waterloo Thermal Conductivity Test
Report**

Thermal Conductivity Measurements for Composite Al – APG

Material

prepared by

Pete Teertstra and J. Richard Culham

Microelectronics Heat Transfer Laboratory

Department of Mechanical Engineering

University of Waterloo

Waterloo, ON N2L 3G1

Canada

for

Shane Flynn

Curtiss-Wright Controls

333 Palladium Drive

Kanata, ON K2V 1A6

December 23, 2004

The Microelectronics Heat Transfer Laboratory (MHTL) performed in-plane effective thermal conductivity measurements for a composite aluminum – annealed pyrolytic graphite (APG) material. This material was provided to the MHTL by Curtis-Wright Controls in the form of a frame, which will be cut apart and used to construct the test samples. Figure 1 shows a schematic of the frame and the regions and number / relative size of the cutout pieces and Figs. 2 and 3 show the frame and pieces after cutting.

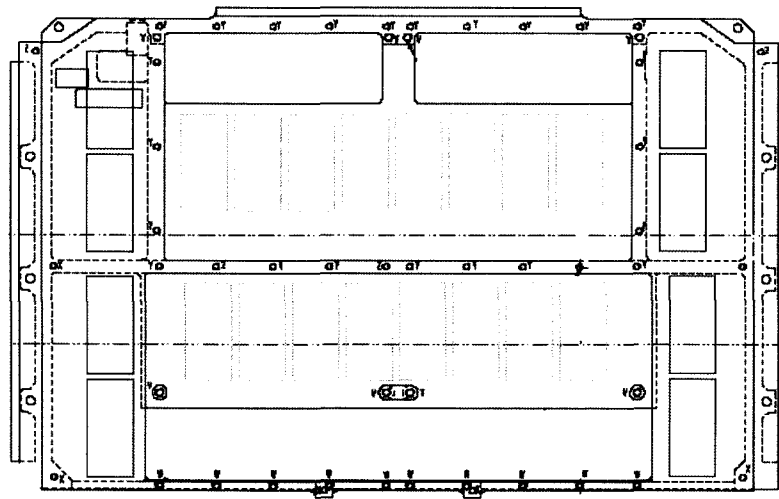


Fig. 1 Schematic of cutout locations for test sample construction

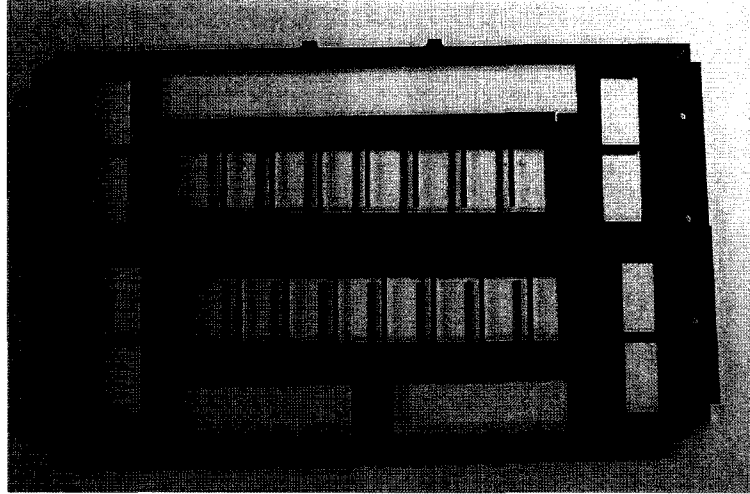


Fig. 2 Frame with test sample cut-outs

The frame was cut in half using a band saw to identify the exact dimensions of the graphite inserts. Then, the sample pieces were cut using a water jet process to the following dimensions:

- 0.120" section thickness – 15 x 25 *mm* (8 pieces)
- 0.063" section thickness – 14 x 25 *mm* (15 pieces)

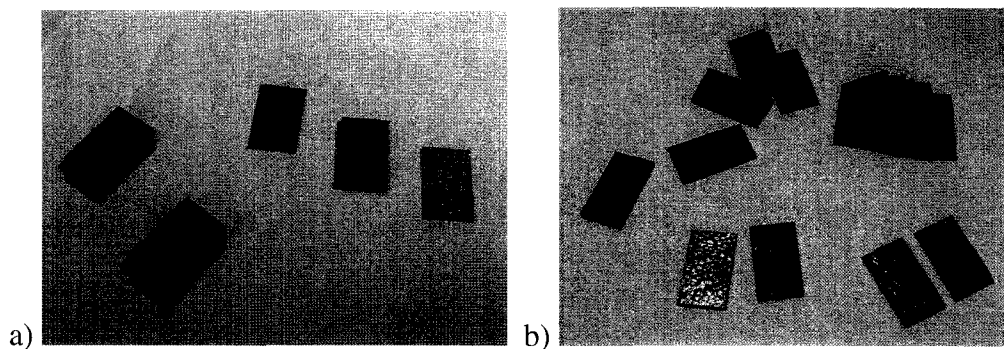


Fig. 3 Test samples, showing de-lamination: a) 0.120" section; b) 0.063" section

The water jet cutting process caused de-lamination of the aluminum and graphite layers in most of the sample pieces. Each of the sample pieces were re-laminated using Loctite cyanoacrylate (Superglue) adhesive prior to assembly of the final test specimen, as shown in Fig. 4.

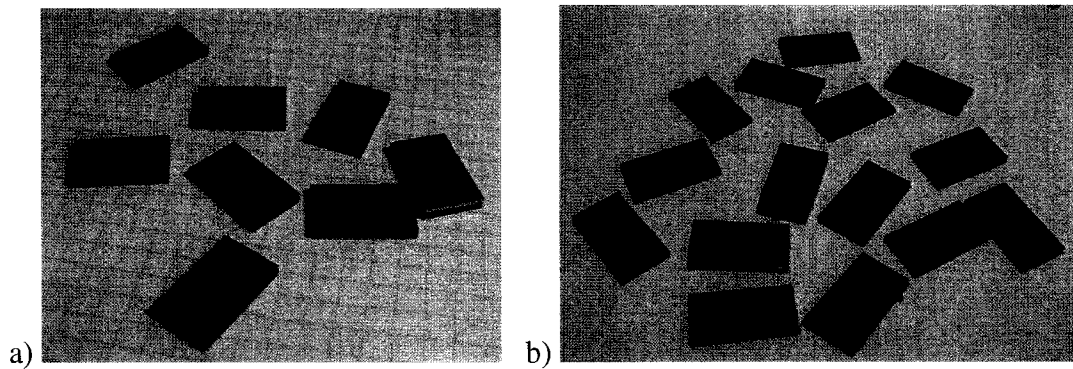


Fig. 4 Test samples after re-laminating: a) 0.120" section; b) 0.063" section

The edges of each of the sample pieces were dressed using a small file to remove burrs left by the cutting process. Then the test samples were assembled by laminating the pieces using Loctite 290 Green threadlocker and clamping in a small vise, as shown in Fig. 5. Once the stacks were assembled and clamped, the adhesive was cured in an oven at approximately 200 °F for 45 minutes.

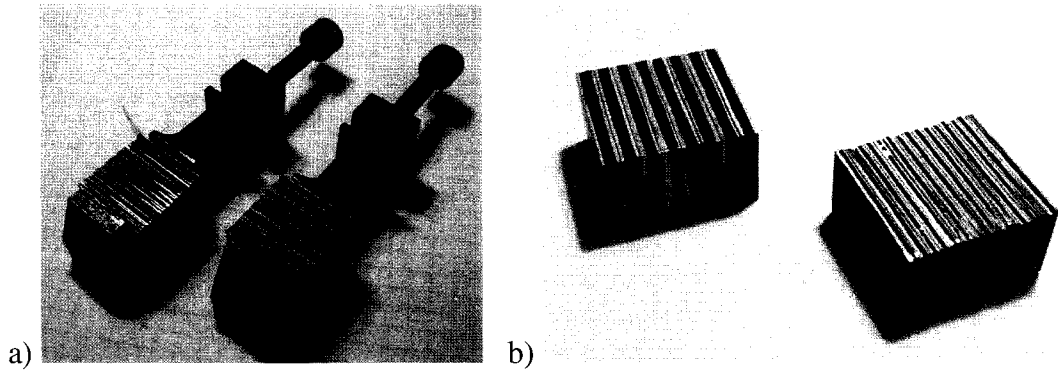


Fig. 5 Test samples: a) assembled and clamped; b) adhesive cured, clamps removed

In order to hold the test samples together during subsequent machining and testing, the stacks were encapsulated in fiberglass resin, using a small round plastic container as a mold, as shown in Fig. 6 a). When the resin had cured, the top and bottom surfaces of the encapsulated samples were fly-cut to reveal the laminate material. For the first set of measurements for each sample, the minimum amount of material was cut to expose the aluminum – graphite material and ensure a flat surface for good thermal contact to the test apparatus. The completed test samples are shown in Fig. 6 b) and dimensions for the samples are given in Fig. 7.

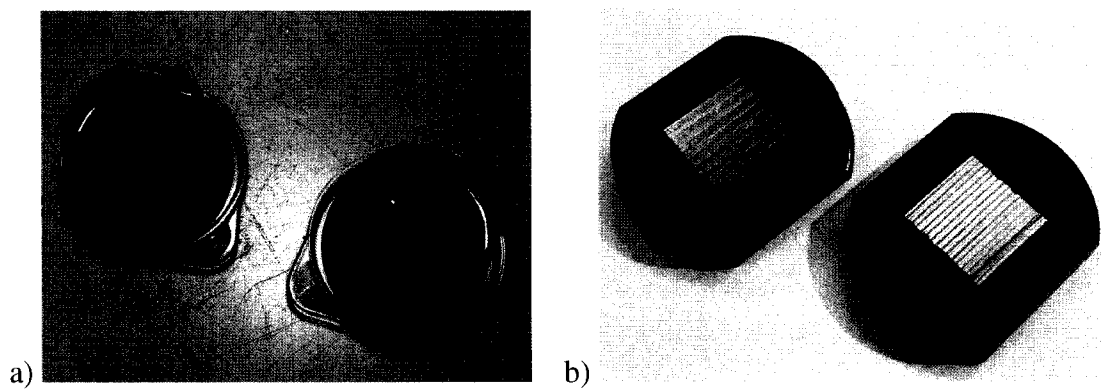


Fig. 6 Test samples: a) encapsulated in fiberglass resin; b) completed

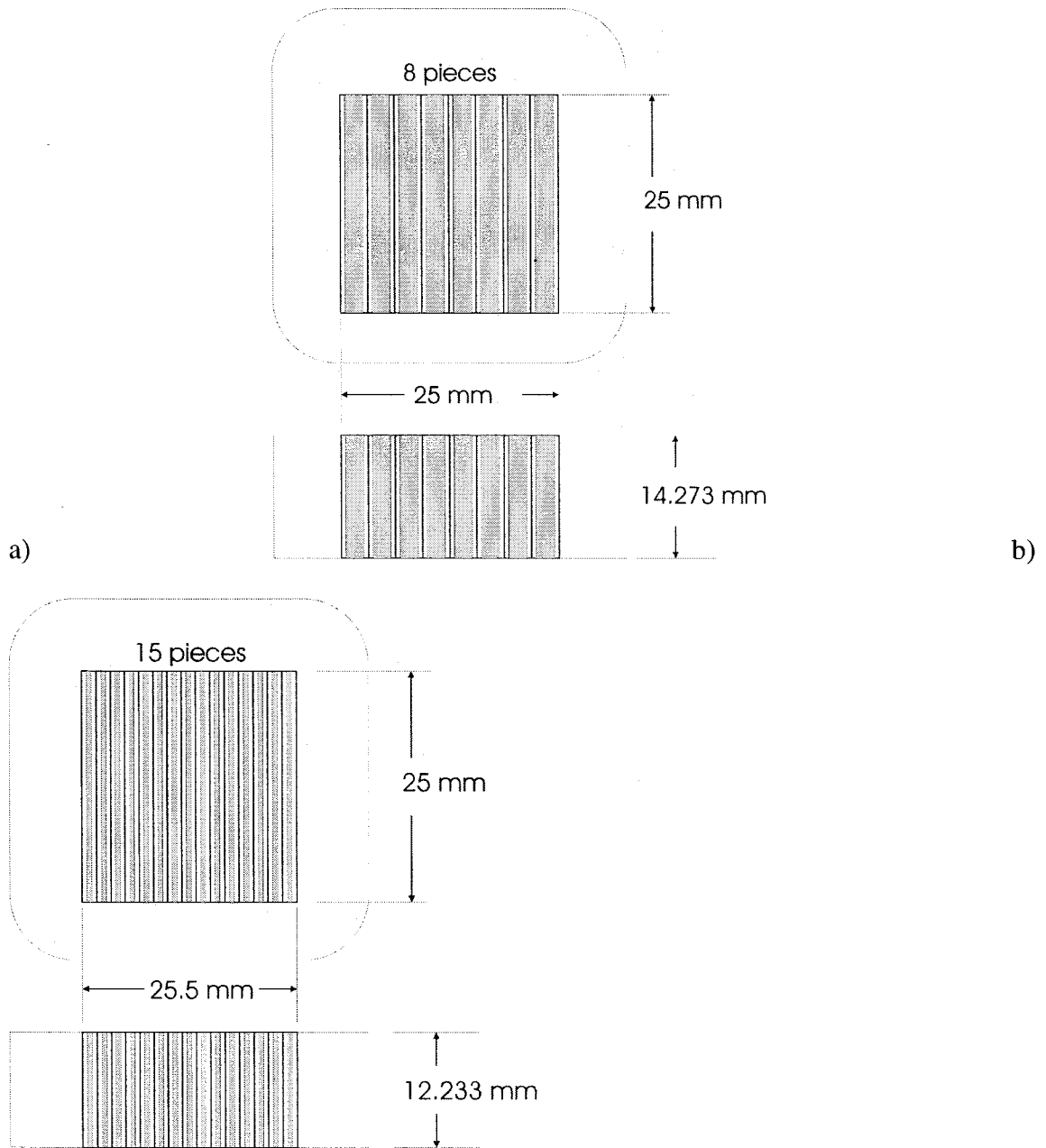


Fig. 7 Schematic of final test sample dimensions: a) 0.120" sample; b) 0.063" sample

Thermal joint resistance was measured in the thermal interface material (TIM) test apparatus at the MHTL under the following test conditions: $T_{\text{joint}} = 50^{\circ}\text{C}$, contact pressure $\approx 100 \text{ psi}$. Figure 8 shows one of the samples under test in the TIM measurement apparatus.

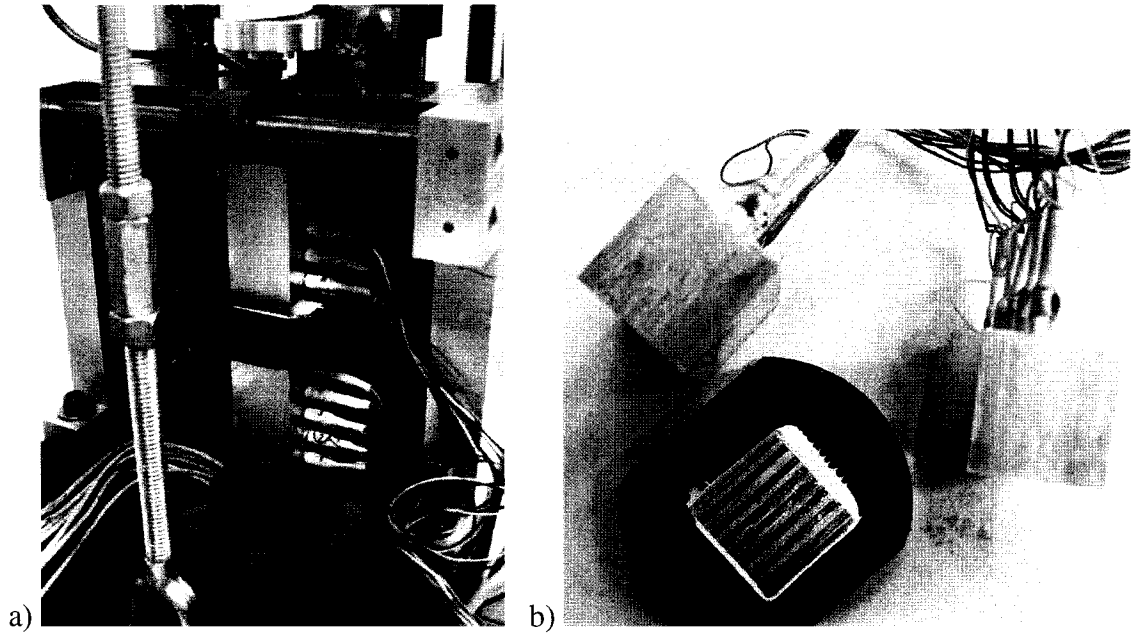


Fig. 8 Testing of composite material sample: a) TIM test apparatus; b) joint with thermal grease applied

In order to minimize the thermal contact resistance between the sample and the heat flux meters of the TIM test apparatus, a thin layer of Dow Corning 340 thermal grease was applied at each of the joints. Figure 8 b) shows the joint with the thermal grease present after the test is completed. The ability of the application method to apply a constant bondline thickness of thermal grease for subsequent tests is validated by performing repeat tests for each of the samples tested.

Due to the high conductivity of the constituent materials in the test sample, the contact resistance between the heat flux meters of the TIM apparatus and the sample cannot be neglected. A test method has been devised whereby the effect of contact resistance at the two joints formed between the sample and the apparatus is reduced from the total resistance. Starting with the as-received thickness of 14.273 mm for the 0.120" sample and 12.233 mm for the 0.063" sample, total joint resistance R_1 is measured. Then the samples are flycut again to reduce the thickness by approximately 1/3 and total joint resistance R_2 is measured. Assuming that the heat conduction in the sample is one-dimensional, the following relationship is used to relate thickness to conductivity:

$$R_1 = \frac{t_1}{k A}, \quad R_2 = \frac{t_2}{k A}$$

where t_1 and t_2 are the sample thickness before and after the second flycut. This methodology leads to the following two equations:

$$2R_c + \frac{t_1}{k A} = R_1$$

$$2R_c + \frac{t_2}{k A} = R_2$$

By assuming that the contact resistance R_c is the same in both tests, the difference of the two equations can be used to determine the effective thermal conductivity of the sample:

$$k = \frac{1}{A} \left(\frac{t_1 - t_2}{R_1 - R_2} \right)$$

where A is the cross sectional area of the sample.

The assumption that the contact resistance R_c is constant in all tests is validated by performing three repeat tests for the 0.120" sample, where the total resistance value varied by less than 3%, as shown in Table 1.

Table 1 Total joint resistance for 0.120" sample – repeat test results

<i>Load</i> (MPa)	<i>Q</i> (W)	ΔT (°C)	R_{tot} (°C/W)
0.717	36.04	4.01	0.111
0.706	33.27	3.88	0.117
0.701	30.14	3.20	0.106

Table 2 presents the test results for total joint resistance for all of the measurements performed on each of the test samples. A full listing of all raw data are presented in the Excel spreadsheet that accompanies this report.

Table 2 Total joint resistance measurements

t (mm)	Load (MPa)	Q (W)	T_{joint} (°C)	ΔT (°C)	R_{tot} (°C/W)
0.120" Sample					
14.273	0.717	36.04	52.0	4.01	0.111
14.273	0.706	33.27	51.6	3.88	0.117
14.273	0.701	30.14	52.2	3.20	0.106
Average	0.708		51.9		0.111
10.053	0.689	30.56	52.4	2.41	0.079
10.053	0.682	29.81	51.6	2.29	0.077
Average	0.685		52.0		0.078
0.063" Sample					
12.233	0.699	31.12	52.4	3.82	0.123
12.233	0.705	31.08	52.1	3.83	0.123
Average	0.702		52.3		0.123
8.025	0.687	27.48	51.6	2.72	0.099
8.025	0.676	28.13	50.1	2.82	0.100
Average	0.681		50.9		0.100

Based on the measured values shown in Table 2, the effective thermal conductivity for the composite material is calculated for each sample.

- 0.120" Sample**

$\Delta t = 4.22 \text{ mm}$

$A = 6.25 \times 10^{-4} \text{ m}^2$

$\Delta R = 0.033 \text{ } ^\circ\text{C/W}$

$k = 202.1 \text{ W/m K}$

$$\Delta t = 4.208 \text{ mm}$$

$$A = 6.37 \times 10^{-4} \text{ m}^2$$

$$\Delta R = 0.023 \text{ }^\circ\text{C}/\text{W}$$

$$k = 282.2 \text{ W}/\text{mK}$$

- **0.063” Sample**

A number of observations and conclusions can be drawn from these measurements.

- Based on these measurements and an assumed conductivity of approximately 180 W/mK for the aluminum in the composite, it is apparent that the thermal conductivity of the graphite in the composite is significantly less than that reported by the manufacturer, i.e. $> 2500 \text{ W}/\text{mK}$. The data suggest that the actual conductivity (in-plane) of the graphite is of order 200 – 300 W/mK .
- The difference between the effective conductivity between the 0.120” and 0.063” samples can be as a result of experimental uncertainty or a real, physical effect. Due to the large effective conductivity of the sample, the instrument was operating near the limit where uncertainties in temperature measurements become a factor. It is also possible that the physical properties of the thinner layer of graphite are different than those of a thicker layer, perhaps as a result of more compression of the material during manufacturing, etc. Future testing using larger thickness sample instrumented with thermocouples to capture the temperature gradient in the material may provide more accurate results.
- When the composite material was de-laminated as a result of the water jet cutting process, it allowed for a close visual inspection of the graphite material. The graphite appeared to be porous, with a flake-like structure rather than a continuous, homogeneous material. This porous structure may account for the decreased thermal conductivity in the steady state testing, which relies on long distances, versus the laser-flash data which considers only a very short distance. A micro-structure analysis using an optical or electron microscope may be useful to better characterize the material.

References

- ¹ Colwell, R., *CPU Power Challenges 1999*, International Symposium on Low Power Electronics and Design, 1999.
- ² Johnson, W., *The Changing Automotive Environment: High-temperature Electronics*, Advanced Packaging Magazine, May, 2004.
- ³ Fitzhugh, Dr. G., Comfort, Dr. R., *Validated Modernization*, Diminishing Manufacturing Sources and Material Shortages Conference, 2000.
- ⁴ Holman, J., *Heat Transfer*, 8th Edition, McGraw-Hill Publishing Company, New York, 1997.
- ⁵ St. Louis, C., *Effects of Random Vibration, Wick Structure and Body Forces on the Capillary Limit of Heat Pipes for Electronics Cooling*, Carleton University Master's Degree Thesis, 2002.
- ⁶ Kelly, *Concise Encyclopedia of Composite Materials*, Pergamon Press, Oxford, 1988.
- ⁷ McNaught, A., Wilkinson, A., *IUPAC Compendium of Chemical Terminology*, 2nd Edition, Blackwell Science, 1997.
- ⁸ *HOPG – Highly Oriented Pyrolytic Graphite*, Structure Probe Inc., West Chester, PA, viewed 11 August 2004, <<http://www.2spi.com/catalog/new/hopgsub.shtml>>.

⁹ Rantala, J., *Pyrolytic Graphite – Thermal Performance by Structure*, Electronics Cooling Magazine, August, 2002.

¹⁰ Osman, M., et al. *Temperature Dependence of the Thermal conductivity of Single-Wall Carbon Nanotubes*, Nanotechnology Vol. 12, 2001.

¹¹ GE Advanced Ceramics, *TC-1050: Heat-Spreaders, Heat Sinks, Thermal Cores*, GE Advanced Ceramics, Cleveland, OH, viewed 13 January 2003, <<http://www.advceramics.com/acc/products/tc1050/>>.

¹² Occhionero, M., et al., *Extremely High Thermal Conductivity Package Components for High Heat Flux Semiconductors, RF/Wireless, and Optoelectronics*, Ceramics Process Systems Corporation, Chartley, MA, 2002

¹³ Taylor, D. L., Groot, H., Ferrier, J., *Thermophysical Properties of 2D Pyrolytic Graphite: A Report to K Technology Corp.*, Thermophysical Properties Research Laboratory, Inc., October, 2000.

¹⁴ Karlsson, L., et al., *Modeling in Welding, Hot Powder Forming, and Casting*, ASM International, Ohio, 1997.

¹⁵ Ogden, T.R., *Thermal Conductivity of Anodic Oxide Coatings on Aluminum*, Naval Ocean Systems Center, Materials Letters, Volume 5, Number 3, February, 1987.

¹⁶ Zhang, S., et al., Evaluation and Finite Element Modeling for New Type of thermal Material – Annealed Pyrolytic Graphite (APG), The 32nd Annual Conference on

Thermal Analysis and Applications - North American Thermal Analysis Society
(NATAS), Williamsburg, VA, 2004.